POLITECNICO DI TORINO

Facoltà di Ingegneria

Corso di Laurea Magistrale in Ingegneria Energetica e Nucleare

Tesi di Laurea di II livello

URBAN AIR CLEANER DESIGN AND FEASIBILITY STUDY

Supervisor: **Candidate:**

Prof. Marco Simonetti   Davide Carlucci

External supervisors:

Prof. Ricard Garcia Valls

2019

(Page intentionally left blank)

TABLE OF CONTENTS

Davide Carlucci

(Page intentionally left blank)

Davide Carlucci

ACKNOWLEDGMENTS

I would like first to express my gratitude for Dr. Sebastià Carrión that with his foundation, Greennova, sponsored and gave the idea for the project. It has been a pleasure to exchange opinions and ambitious visions with a such inspiring and motivated person like him.

I would like to thank my supervisors Prof. Ricard Garcia Valls, Dr. Adrianna Nogalska and all the members of the MEMTEC (CTQC, Tarragona) for having accepted and supported me in their research group during these months.

Likewise, I would like to acknowledge Prof. Marco Simonetti for his help and his patience, even if thousands of kilometers far. In particular, his kindness and availability have been fundamental for the elaboration of this Thesis.

Davide Carlucci

ABSTRACT

In the past decades, the rising levels of air pollution in urban areas are threatening the natural environment and the human health. This Thesis focuses on the development (CAD design) and feasibility investigation (evaluation of introduced losses) of a prototype device for passive air cleaning, after an initial review of the existing technologies in the field. The guideline of the project has been to use the device mounted on cars, taking advantage of their motion for the passive suction of the external air. To give the work a more practical resonance, the study has been based on the Barcelona urban area framework. Prior to the mentioned steps, an evaluation on the air pollution levels in Barcelona city, through institutional data processing via MATLAB, has been carried. The analysis, besides proving a seasonality of the pollution problem, showed that the regulatory limits are often exceeded, along the seven monitored months. The best technology, for the removal of a wide range of compounds from the air, is the impregnated activated carbon, in pellets or granulated, that uses the principle of chemical adsorption. After designing the first shape of the prototype, it has been firstly simulated through a 2D COMSOL model to estimate and compare the aerodynamic losses introduced by the presence of the device while mounted in different positions, like roof or hood of the car. The study lead to the conclusion that the hood position has to be preferred, for its smaller drag induced and enhanced air flow rate. Analysing the flow field other optimization are brought that implied the shape change of the device, the position of the activated carbon and the addition of some deflectors. Once determined the best position, the same configuration has been simulated in 3D. An estimation of the average cars emissions in province of Barcelona, together with the simulations results, in terms of drag losses introduced and air flow rate generated, have been used to evaluate the feasibility of the device. It emerged that, with the actual configuration, the ratio airflow generated vs drag losses is not high enough to justify the use of the device. Further experimental tests on the filtering media real parameters, together with an improvement of the device shape, must be done in the future to re-evaluate the feasibility of the project.

Davide Carlucci

1   CHAPTER 1: INTORDUCTION TO AIR POLLUTION

Air pollution is considered as the occurrence in the atmosphere of gases and particles at levels higher (noxious emissions), or lower (gas depletion), than the natural ones. The atmosphere composition is not constant across the eras and is highly interrelated to many natural parameters, such as Earth surface temperature, volcanic eruptions, sunray intensity and so on. Despite this slow variability along age times, big changes have been measured within around a century in coincidence with the advent of the industrial revolution. The strict correlation between these two events emphasizes the human responsibility in the air pollution phenomenon.

Figure 1 Pollution cloud over Barcelona, Spain (picture taken from *El País* [1])

The vision of smog clouds (Figure 1) that overlooks the urban areas supports the already evident and agreed thesis of the anthropogenic source of air pollution. The harmfulness determined by compounds imbalance affects both the environment and human health, leading to tangible transformations in biosphere equilibrium. *"Ambient (outdoor air pollution) in both cities and rural areas was estimated to cause 4.2 million premature deaths worldwide in 2016"* [2] according to World Health Organization.

Davide Carlucci

1.1 Air pollutants categories

The air pollutants are produced by different sources and are usually divided into primary and secondary pollutants. This distinction is necessary because of the different nature and formation of the contaminant belonging to the two different categories: the primary pollutants are directly emitted in the atmosphere by human activities as wastes of mainly factories, power plants, animal agriculture, heating systems and transportation, while the secondary pollutants are generally not directly released but are byproducts of the interaction between the primary pollutants with other atmospheric compounds and/or solar radiation.

1.1.1 Primary pollutants

The main primary pollutants, whose toxicity has been studied and attested, are listed.

- **Carbon dioxide (CO_2)**: carbon dioxide is a gas whose presence in the atmosphere is justified by both natural and anthropogenic sources. Before the industrial era, its concentration in the air has been regulated mainly by the photosynthesis and respiration (carbon cycle). Nowadays an imbalance in this natural cycle has been created by the big emission in atmosphere due to humans' activities. Hydrocarbons combustion has been found to be the main source of anthropogenic emission. Its effects on the environment are much heavier than the adverse effects on human health, making it the most-significant greenhouse gas.

- **Carbon monoxide (CO)**: it is toxic, harmful for health and is less occurrent than carbon dioxide. It is released by incomplete combustion of fossil fuels.

- **Nitrogen oxides (NO_x)**: more than a single pollutant this is a family of pollutants because it comprises the most well-know and common NO_2 and NO, among other five compounds [3] (N_2O, N_2O_3, N_2O_4, N_2O_5, N_4O_6). The nitrogen oxides are mainly produced in combustion processes in two different ways, depending on the origin of the nitrogen. In fact, the so-called *fuel NO_x* is being emitted due to the presence of the nitrogen in the fuel itself, this happens in coal and oil, which during the combustion reaches the flue gas. The other one, the *thermal NO_x*, it is usually formed in high temperature combustion, as the one that takes place inside diesel engines, even while burning fuels that do not contain relevant

quantities of nitrogen. Due to the high temperature, reactions between atmospheric nitrogen and oxygen occur causing the formation of nitrogen oxides [4].

- **Sulfur Oxides (SO$_x$):** also this pollutant should be better defined as a group of pollutants whose most common one is SO$_2$ (sulfur dioxide). The sulfur dioxide in the atmosphere is mostly release by volcanoes eruption. High concentrations in urban areas are usually due to human activities like coal burning for energy production, ores smelting and vehicles emissions [5].

- **Particulate matter (PM):** they are inhalable particles characterized by a very small size divided into PM2.5, with diameter under 2.5 µm, and PM10, with diameter under 10 µm comprising so also the finer PM2.5. Particulate matter is composed by several substances as sulphate, nitrates, ammonia, sodium chloride, black carbon, mineral dust and water. Their presence in the air is due to flue gases of vehicle engines and combustion of fossil fuels in general.

- **Volatile organic compounds (VOCs):** they are organic compounds with high vapor pressure, at ambient condition, that let them evaporate easily being so extremely volatile. Paintings, coating are hugely responsible for benzene, formaldehyde and other VOCs release as well as the combustion of fossil fuels too. Diesel and petrol, for example, contain hundreds of hydrocarbons that are in the category of VOCs. They are the major responsible, together with NOx, for the formation ground-level ozone.

1.1.2 Secondary pollutants

The secondary pollutants are rarely emitted directly into the atmosphere, but they are formed when the primary pollutants (or precursors), especially NO$_x$, SO$_x$ and VOCs, are exposed to sunrays like UVs. This process, known as photo-oxidation, generates the so-called photochemical smog.

- **Ground-level Ozone (O$_3$):** it is formed by the nitrogen oxides. It is called ground level, or tropospheric, ozone to differentiate it from the stratospheric one whose role is important for the absorption of huge amounts of UV radiation, dangerous for the biosphere. When presents in lower part of the atmosphere it is

considered a pollutant harmful for human health and environment. Its main precursors are NO_x, CO and VOCs.

- **Sulfuric acid (H_2SO_4) and Nitric acid (HNO_3):** these compounds have nitrogen oxides and sulfur oxides as precursors when they react with the atmospheric water creating the famous acid rain. Their hazardousness involves both the environment and the human health.

These are just the main pollutants, considered mainly for their wide presence at global level; other minor compounds, despite the even bigger relative harmfulness, are not cited here for brevity reasons.

1.2 Adverse effects and WHO guidelines

Tenths of statistical and epidemiological studies have been carried on the above-mentioned compounds to obtain evidence on the adverse effects on human health. Since the presence of only a single isolated pollutant is seldom possible, the coexistence of several compounds makes more difficult to determine accurate conclusions.

Table 1 WHO guidelines and adverse effects for the main pollutants [6]

Pollutant	Guideline	Adverse effects
Particulate Matter	**PM2.5** • 10 µg/m^3 annual mean • 25 µg/m^3 24-hour mean **PM10** • 20 µg/m^3 annual mean • 50 µg/m^3 24-hour mean	Ischemic events Arrythmia
Ozone	100 µg/m^3 8-hour mean	Breathing problems Trigger asthma Reduced lung function Lungs morbidity increased
Nitrogen Dioxide	40 µg/m^3 annual mean 200 µg/m^3 1-hour mean	Bronchitis in asthmatic children Reduced lung function
Sulfur Dioxide	20 µg/m^3 24-hour mean 500 µg/m^3 10-minute mean	Cardiac diseases increase Reduced lung function Eyes irritation Inflammation of respiratory tract Asthma aggravation

Davide Carlucci

Although direct quantitative correlation between the exposure and the effects cannot be formulated, the World Health Organization [6] attempted to set some averaged limit values for some of the main pollutants (Table 1), with the aim to reduce the risk for people. As it can be seen, the WHO fixes guidelines only for certain pollutants, considering mainly their hazardousness and recurrence in the measurements.

2 CHAPTER 2: AIR QUALITY EVALUATION IN BARCELONA

The work of this Thesis is centered on the case study of the city of Barcelona in Spain, as already mentioned. Understanding which contaminants, and in which measure, are mainly present and monitored in city of Barcelona is necessary to determine the characteristics that the capturing device needs to have. Furthermore, it has relevance to grasp the pollutant limits established by the local administration, by comparison with the WHO guidelines.

2.1 Catalan Air Quality Index

The *Generalitat de Catalunya* (Government of Catalonia) created in 1995 an index called ICQA [7] (*Índex Català de Qualitat de l'Aire*, that stands for *Catalan Air Quality Index*) to quantify in a single parameter, easy to understand, the quality of the air according to their specific guidelines.

VALORS D'IMMISSIÓ	ICQA	100 a 50	49 a 0	-1 a -50	-51 a -100
	O3 1h (µg/m³)	0 - 110	111 - 180	181 - 240	> 241
	PM10 24 h (µg/m³)	0 - 35	36 - 50	51 - 75	> 76
	CO 8h (mg/m³)	0 - 5	6 - 10	11 - 15	> 16
	SO2 1h (µg/m³)	0 - 200	201 - 350	351 - 500	> 501
	NO2 1h (µg/m³)	0 - 90	91 - 200	201 - 400	> 401

QUALITAT DE L'AIRE	BONA	REGULAR	POBRE
ICQA	≥ 50	0 - 49	< 0

Figure 2 ICQA value for each pollutant [7]

The Figure 2 shows the index attributed to each pollutant based on the concentration level: the limit values (green column) are in general stricter than the ones recommended by the WHO. Anyway, it should be considered that some values are averaged on different time length. The overall ICQA is obtained by the lowest score registered among the five pollutants considered.

Davide Carlucci

2.2 Monitoring stations

The pollutants concentration values are important to have a deeper idea on the real entity of the problem that the locals are facing.
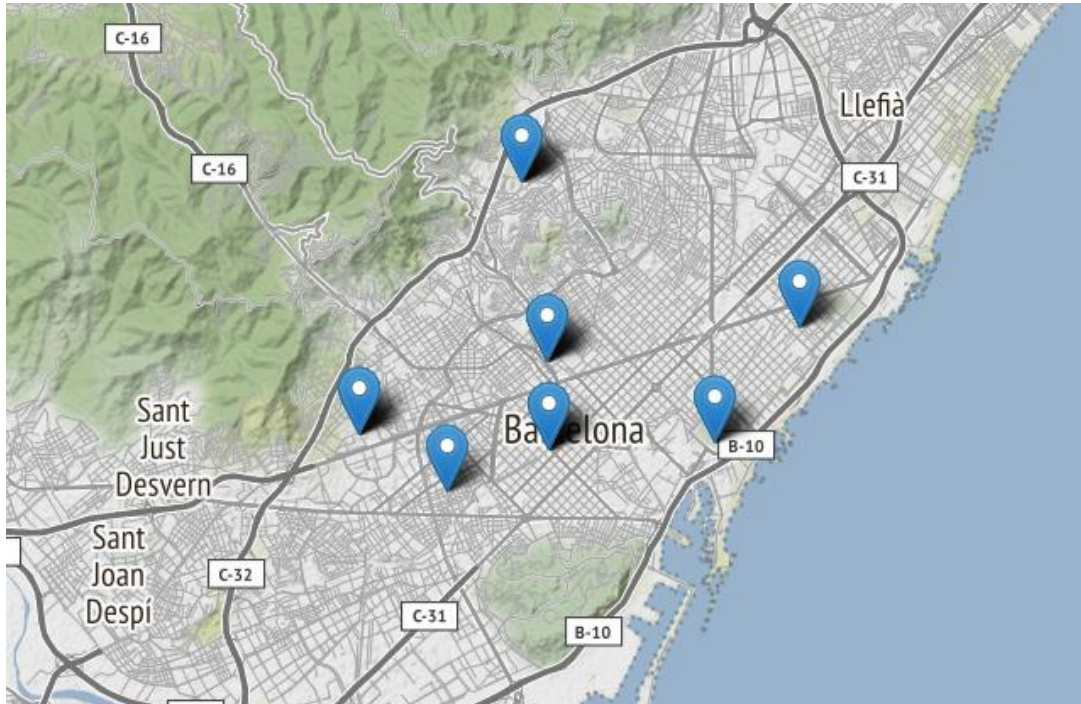

Figure 3 Location of the monitoring station in Barcelona urban area (Observ Fabric exact position is missing)

Various *air quality measure stations*, displaced along strategic spot of the town (Figure 3), sample the air 24/7 generating hourly averaged data. There are eight monitoring stations (Table 2) in the town that are able to measure the level of only three air pollutants: ozone (O_3), nitrogen dioxide (NO_2) and coarse particulate matter (PM_{10}). Some stations can measure all the mentioned pollutants, but three of them (Sants, Ciutadella, Poblenou) lack of the technology to detect ozone and/or particulate matter; nitrogen dioxide sampling is assured in every station.

Davide Carlucci

MONITORING STATION	O₃	NO₂	PM10
Barcelona - Sants	✗	✓	✗
Barcelona - Eixample	✓	✓	✓
Barcelona - Gràcia	✓	✓	✓
Barcelona - Ciutadella	✓	✓	✗
Barcelona - Vall Hebron	✓	✓	✓
Barcelona - Palau Reial	✓	✓	✓
Barcelona - Poblenou	✗	✓	✓
Barcelona - Observ Fabra	✓	✓	✓

2.3   Air quality data import and manipulation

The *Ajuntament de Barcelona*, the town hall of the Catalan city, provides monthly the data collected through its website [8] . The files are published at the end of every month in *.csv* format. Historical data start since June 11th, 2018.
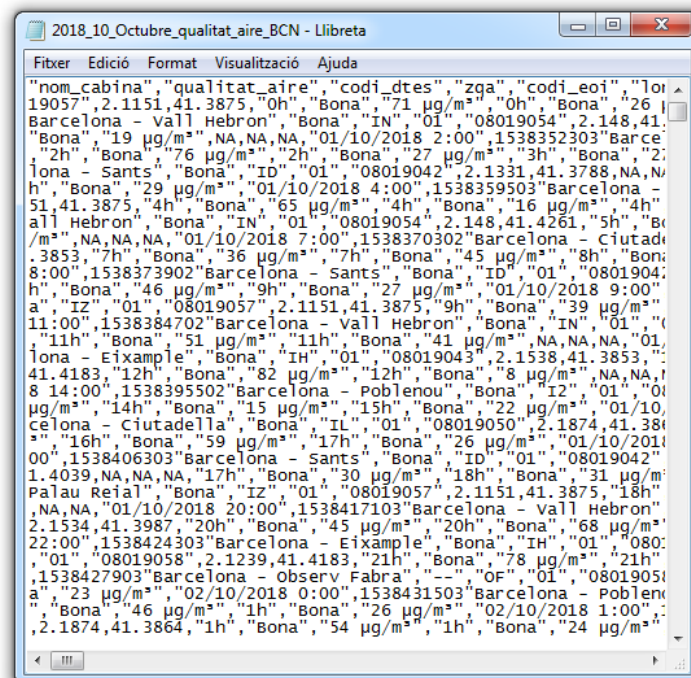

Figure 4 Original format of the raw data extracted by the monitoring stations samples

The creation of a Matlab script for the analysis of the files is strictly necessary since the values are tabulated in a not easy, tough intuitive, way, as shown in Figure 4. The work led to writing a script that is able to read the file, import the data, manipulate the imported arrays and generate plots while recognizing and handling the exceptions. In fact, it has been observed the presence of "NA" and "--" values among the numerical data: this problem is supposed to occur when the sampling station is under maintenance or when it fails to the detect the pollutant amount. The script is devoted also to distinguish the format of the values, eliminating the units ($\mu g/m^3$), transforming the generated strings arrays into double precision arrays, letting so the data to be sorted by station of origin, made understandable and ready to be plotted for further analysis. The commented script is reported at the end of this Thesis, in the Appendix A.

2.4 Air quality data analysis

The historical data analyzed are the ones available on the mentioned website to date. The period considered starts in July 2018 and ends in January 2019. The following months contains errors, due to some format issue. Anyway, the seven months of data processed can provide enough information for the purpose of this Thesis: the cumulative number of hours amounts to 38625 among all the monitoring stations.
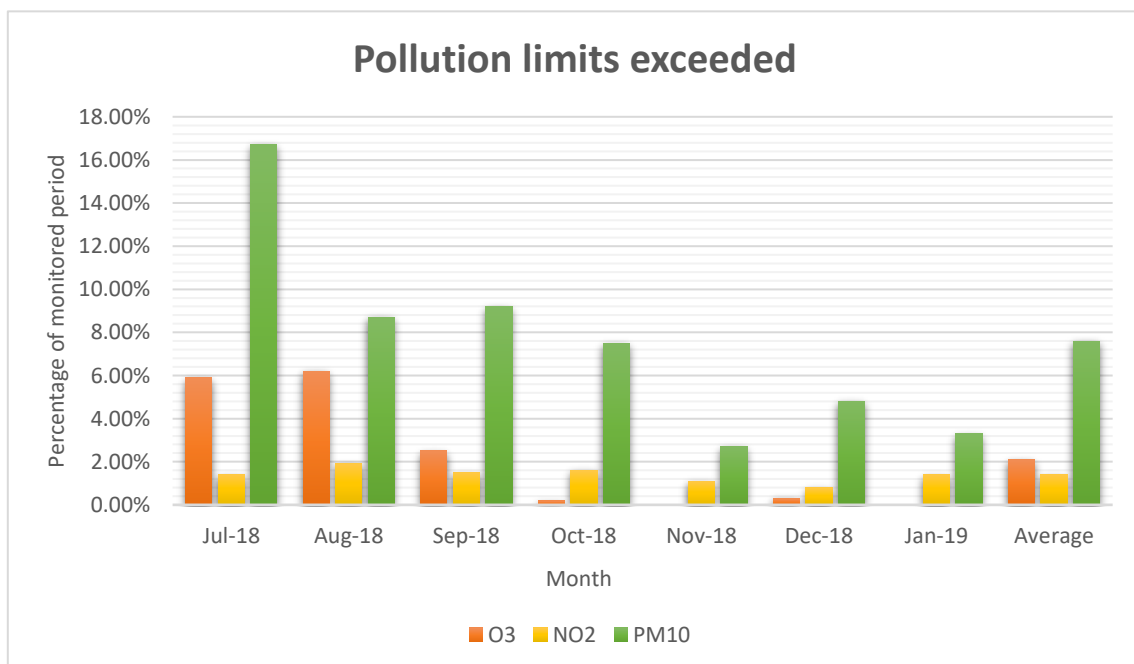

Figure 5 Percentage of hours monitored with pollutants limits exceed (period 07/18-01/19)

Davide Carlucci

Examining the data (Figure 5), it came out how the pollution levels for particulate matter are exceeded more often during the summer period than in colder months. This behavior was expected for a town in the geographical position of Barcelona, since the particles tend to settle during rainy season (late autumn and winter) leading to a decrease in the measured concentration.

The gaseous pollutants, because of their nature, are less affected by the settling process. Despite this, the ozone levels show a big contraction approaching the winter. The reduction, in fact, is not due to an increase in precipitation frequency but rather to a decrease in solar radiation. Indeed, being the tropospheric ozone a secondary pollutant, it needs for high level of solar radiation to be formed.

Anyway, the most important result regards the nitrogen dioxide level: it appears to be quite constant along all the months evaluated. Due to this worrying behavior, major attention has to be addressed to this gaseous contaminant.

Davide Carlucci

3 CHAPTER 3: AIR CLEANING METHODS, A REVIEW

From the previous analysis on the pollutants, it emerges clearly that actions are needed to tackle the air pollution. Gases and particles capturing is done through different mechanism, and so technologies, because of their different properties, in particular the dimension. In this Chapter the various principles and technologies for capturing each pollutant will be investigated.

3.1 Particles capture

3.1.1 Particles capturing principles

To find the proper particle filtration technology to be installed in our device, the main effects exploited for particles capturing are reviewed first [9]:

- The **sieve effect** (Figure 6): it is one most commonly applied in air filters. The principle of the sieve effect is very simple: the particle is larger than the gap between the media fibers and therefore gets trapped.
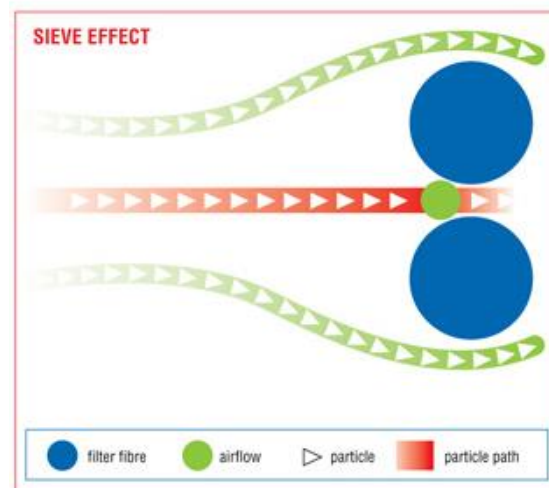

Figure 6 Sieve effect [9]

- The inertial mass effect (Figure 7): this principle occurs if the particles have substantial mass and therefore big inertia. The particles that arrive at high velocity collides with the media fiber and is trapped, instead of being deflected with the airflow.

Davide Carlucci
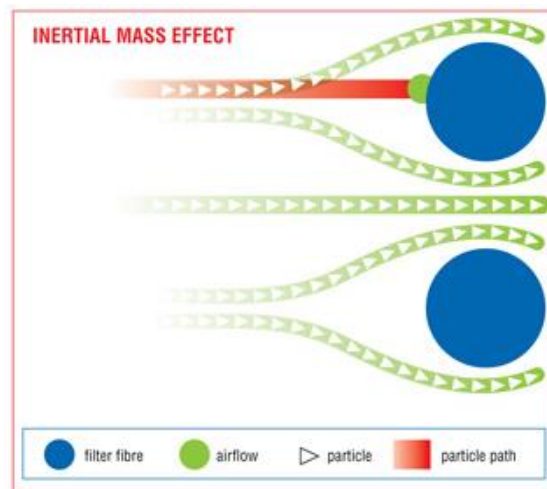
Figure 7 Inertial mass effect [9]

- The interception effect (Figure 8): the fact that particles exert forces of attraction on each other is crucial for this method. The larger media fibers can attract the relatively small dust particles. Once the particles have been intercepted, they remain stuck between the media fibers.
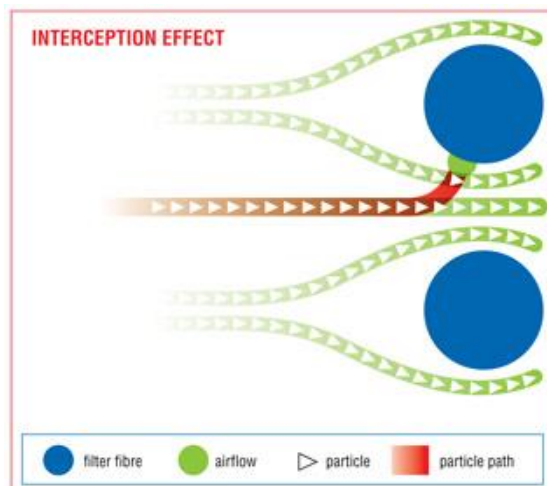

Figure 8 Interception effect [9]

- The diffusion effect (Figure 9): particularly small particles often pursue an irregular path. This phenomenon is referred to as Brownian motion. The path that the particles follow may digress from that of the airflow, so the Brownian motion increases the chances of the particle colliding with the media fibers.
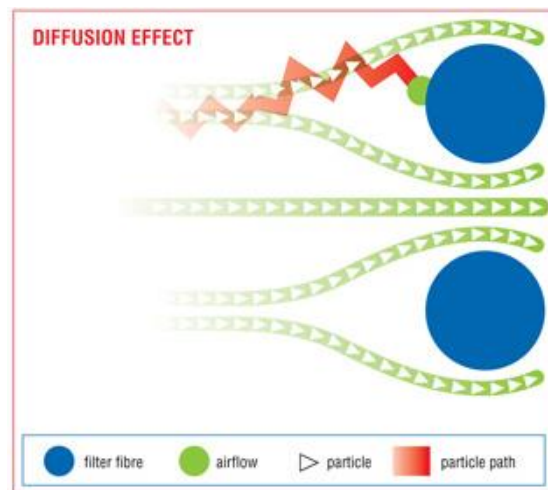

Figure 9 Diffusion effect [9]

3.1.2 Particles capturing technology – HEPA filters

Air purification is a process widely used in HVAC system to decontaminate the inflow air in buildings from dusts, pollen and especially particles. The main technology used is based on the HEPA filters: an acronym that stands for High Efficiency Particulate Air. HEPA was initially commercialized in the 1950s, and the original term became a registered trademark and later a generic term for highly efficient filters. Their efficiency, sometimes called fractional efficiency, is defined as the discrete measure of the number of particles of a specific size downstream of a filter compared to a measure of the number of particles of the same size upstream of the filter [10]. The arrestance, instead, is the ratio between the number of particles trapped and the particles at which the filter is exposed.
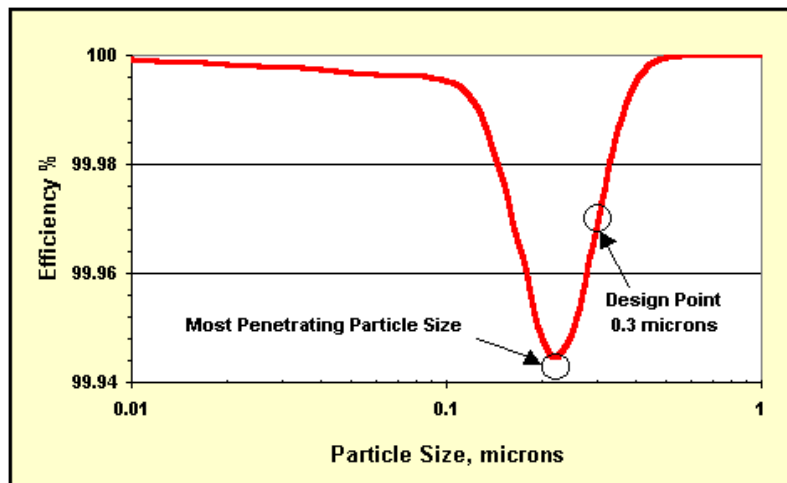
Figure 10 Efficiency of HEPA filters at different particle size

The US standard (DOE-STD-3020-2015) requires HEPA filter to be capable of removing 99.97% of contaminant particles larger than 0.3 μm in diameter. The diameter of 0.3 μm is not a random number but represents the particle size most difficult to trap because of the mechanism involved during filtration. This means that this kind of filters will face a higher penetration for particles of around 0.3 μm, as shown in Figure 10, but still having very high efficiency with values always larger than 99.94%.
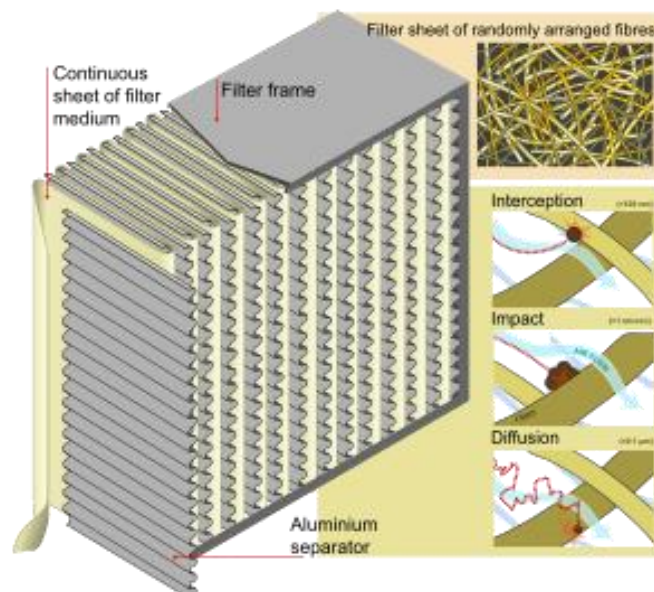
Figure 11 Typical HEPA filters cross section

HEPA filters are made of very fine glass threads with a diameter of less than 1 µm that give to these filters a very high porosity. The filter medium is bended several times, to increase the surface area and reduce the pressure drop. The sheets can be held in position thanks to the interposition of aluminum separators (Figure 11).

3.1.3 HEPA filters rating

The capability of a filter to capture particles is commonly measured through the MERV (Minimum Efficiency Reporting Value) scale rather than the efficiency alone.

| MERV Rating | Minimum % of particles trapped | | |
| | "PM 2.5 Zone" | | |
	0.3 - 1.0 Microns	1.0 - 3.0 Microns	3.0 - 10.0 Microns
MERV-16	>95%	>95%	>95%
MERV-15	>85%	>90%	>95%
MERV-14	>75%	>90%	>95%
MERV-13	>50%	>85%	>90%
MERV-12	>35%	>80%	>90%
MERV-11	>20%	>65%	>85%
MERV-10	-	>50%	>80%
MERV-9	-	>35%	>75%
MERV-8	-	>20%	>70%
MERV-7	-	-	>50%
MERV-6	-	-	>35%
MERV-5	-	-	>20%
MERV-4	-	-	<20%
MERV-3	-	-	<20%
MERV-2	-	-	<20%
MERV-1	-	-	<20%

Figure 12 MERV rating scale for air filters [11]

This measurement scale (Figure 12), created by ASHRAE in 1987, ranges from 1 (low effectiveness) to 16 (best filtration performance) [11]. The capturing efficiency highly depends on the particle size, so it comes that the fractional efficiency is not a constant value as already shown in Figure 10.

Davide Carlucci

Strangely the fractional efficiency-particle diameter dependence is neither monotonic, as one could expect.
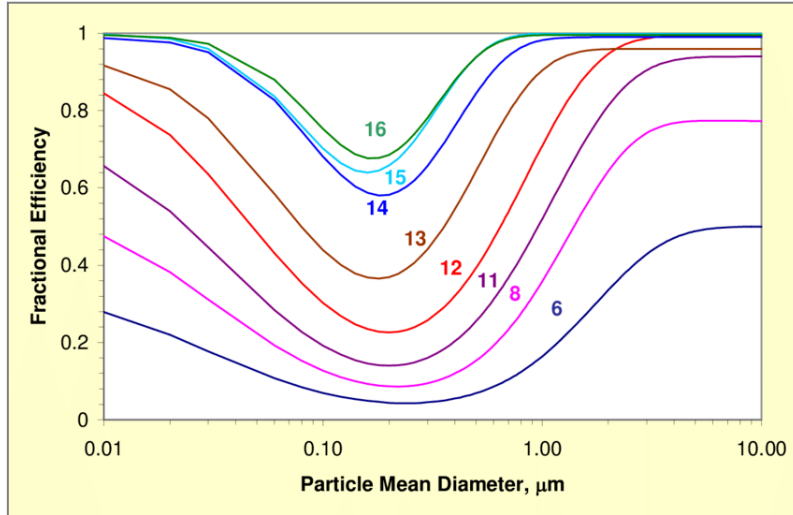
Figure 13 Fractional efficiency of different MERV rated filters [12]

As can be seen from Figure 13 [12], the lowest efficiency occurs between 0.1 and 0.3 μm of particle size. This is due to the fact that the trapping weight of the capturing mechanisms for particles of different size varies with the particle size itself (Figure 14).
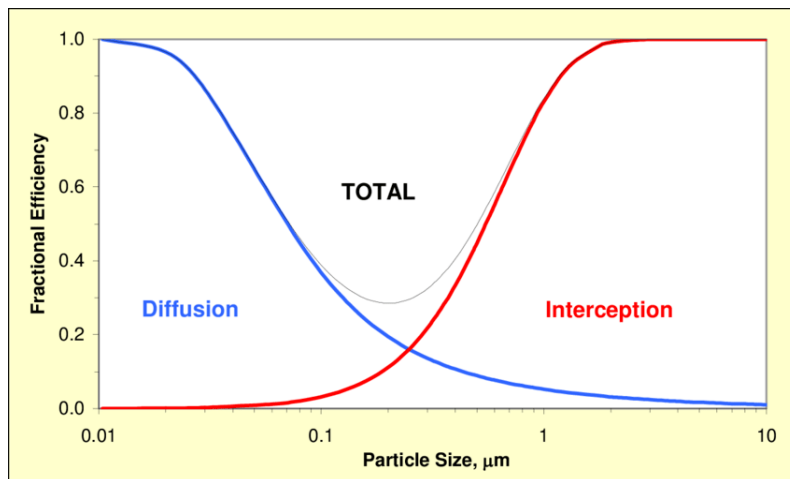

Figure 14 Generalized performance curve for a MERV 15 filter showing components [12]

Davide Carlucci

3.2 Gases capture

3.2.1 Gases capturing technology – Activated carbon

The activated carbon, or activated charcoal, is another important material in air filtration thanks to its ability to collect contaminants even smaller than the ones trapped by common filters. Its production starts with the thermal elimination (pyrolysis) of volatile compounds from materials rich in carbon such as wood, coal or coconut shells, followed by an activation process [13].
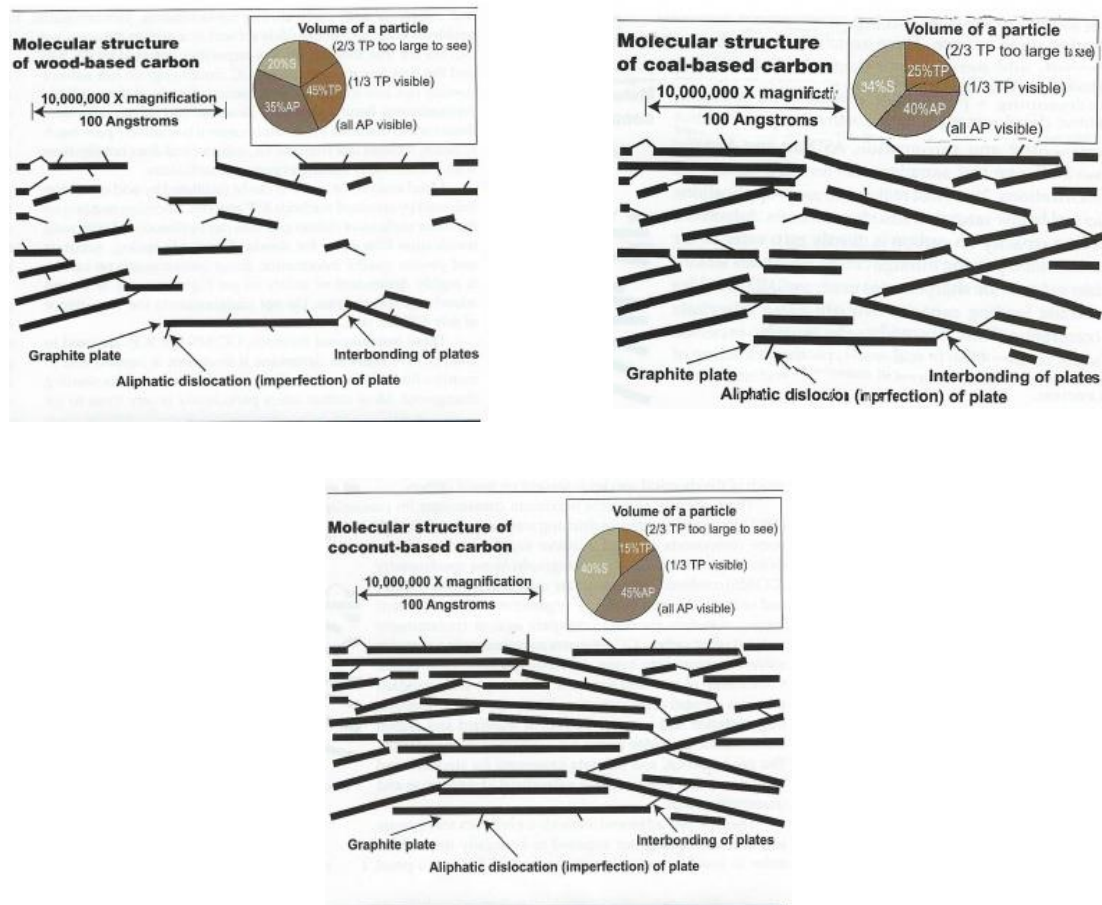
Figure 15 Activated charcoal structure based on raw material origin [14]

The origin of constituents determines the porous dimension (Figure 15) and so the major capturing effectiveness going from bigger porous size of wood-based to the smaller one of the coconut-based, explaining so why the latter is the most used one [14]. Smaller porous size in fact enhances the adsorption in the carbon structure letting the charcoal trap smaller molecules.

Davide Carlucci

3.2.1.1 Activation methods

The charcoal obtained after the pyrolysis needs to be activated in order to develop an interconnected series of cavities or pores inside its structure [15] which gives the material a great internal surface area that is the clue for its adsorption property. There are two main ways to activate the charcoal, with their advantages and drawbacks.

- **Gas Treatment:** The activation of carbon can be done directly through heating in a chamber while gas is pumped in. This exposes it to oxygen for oxidization purposes. When oxidized, the active carbon is susceptible to adsorption, the process of surface bonding for chemicals—the very thing that makes activated carbon so good for filtering waste and toxic chemicals out of liquids and gases. For physical gas treatment, the carbonization pyrolysis process must take place in an inert environment at 600-900 degrees Celsius. Then, an oxygenated gas is pumped into the environment and heated between 900 and 1200 degrees Celsius, causing the oxygen to bond to the carbon's surface [16].

- **Chemical Treatment:** In chemical treatment, the process is slightly different from the gas activation of carbon. For one, carbonization and chemical activation occur simultaneously. A bath of acid, base or other chemicals is prepared and the material submerged. The bath is then heated to temperatures of 450-900 degrees Celsius, much less than the heat needed for gas activation. The carbonaceous material is carbonized and then activated, all at a much quicker pace than gas activation. However, some heating processes cause trace elements from the bath to adsorb to the carbon, which can result in impure or ineffective active.

3.2.1.2 Grain size

The average grain size is another very important factor to be taken into account when choosing the charcoal. Different sizes determine the suitability for different applications and are strictly related to pressure drop and replacement timing [13].

- **Powdered activated carbon (PAC):** Powdered activated carbon consists of fine particles capable of passing through an 80-mesh sieve, being so smaller than 0.177 mm [17]. PAC is particularly suited to applications with a high flow rate but cannot be recycled, so it is not the best choice for applications that use a great deal of activated carbon.

- **Granular activated carbon (GAC):** The next size up, granular activated carbon has a proportionately smaller external surface area than PAC. Smaller GAC is particularly suited to liquid phase applications, while larger GAC is better for vapors and gases. GAC is recyclable, making it advantageous over PAC for applications that use a lot of activated carbon.

- **Extruded activated carbon (EAC):** PAC can be mixed with a binder and formed into cylindrical pellets known as extruded activated carbon. Activation catalysts can also be added to develop a specific pore structure. EAC creates only minimal dust and has a very high mechanical strength but a low pressure drop, making it ideal for gas phase applications.

3.2.2   Gases capturing principles

3.2.2.1   Adsorption

The method widely exploited for gases capture is the adsorption. Adsorption is the attachment or adhesion of atoms, ions and molecules (adsorbates) from a gaseous, liquid or solution medium onto the surface of an adsorbent, the activated carbon in this case [18]. As mentioned, the porosity of activated carbons offers an enormous porosity and surface ($\sim$1000 m^2/g) [19] on which this phenomenon can take place. Adsorption occurs in pores slightly larger than the molecules that are being adsorbed, which is why it is very important to match the molecule diameter that have to be adsorbed with the pore size of the activated carbon. These molecules are then trapped within the carbon's internal pore structure by Van der Waals Forces (physisorption) or other bonds of attraction (chemisorption/chemical adsorption) and accumulate onto a solid surface [20].

3.3   Filtering media selection

The air pollutants have different origin and features between each other (some are gaseous while others are particles), so finding the best technology to deal with all of them is not an easy task. The HEPA filters have excellent performances especially in particles trapping, like the particulate matter, but they lack of effectiveness in gaseous compounds removal. On the other hand, the use of activated carbon assures efficacy in

capturing a wider range of substances, even gaseous. After these considerations it comes clear that the use of adsorption trough activated carbon is essential.

More precisely, the best mechanism to be used for our purposes is the chemisorption. The activated carbon, in order for the chemical adsorption to take place, needs a supplementary chemical treatment called impregnation. The impregnation consists simply in covering the carbon surface with another substance that has affinity with the compounds that need to be captured. In general for aggressive atmospheric pollutants, such as NO_x, impregnation with alkalis or amines.

The company ChiemiVall from Castellbisbal (Barcelona) kindly provided us with two different impregnated activated carbons, to be used in the testing phase of this project: VAPACID PELLET and 940 TEDA.

- The VAPACID PELLET is composed by activated carbon pellets, with a diameter of 4 mm, impregnated with an alkali.
- The 940 TEDA is made of activated bituminous carbon pellets, with a diameter of 4 mm, impregnated with Triethylenediamine (also called TEDA).

However, the use of a HEPA filter, in combination with the activated carbon, has not be excluded totally because it could be used upstream to extend the lifetime of the activated carbon, by removing the particles for a better adsorption of the gases. Anyway, in the following simulations the presence of the HEPA filter will not be considered because of the higher pressure drop that would be introduced, decreasing the overall performance of the system.

Davide Carlucci

4   CHAPTER 4: 2D SIMULATIONS

Simulations are carried to study the response of the system (car + device) when the external stress and constraints are applied. The aim is to determine the proper position of the device on the car and check the effectiveness of the device design. This is done by analyzing four main indicators: the drag coefficient, the total frontal area, the air flow rate in the device and the pressure drop across it. The reason of choosing these values has to be found in their importance in the fuel economy of the car and in the performance of the device.

Their definition, units and explanation are listed:

- Drag coefficient (C_d) [-]: it is a dimensionless value used to calculate the drag force acting on a body that has relative non-zero speed in respect to a fluid. In automotive engineering is usually taken as constant in certain speed ranges even if it is dependent on the Reynolds number.
- Frontal area (A)[m]: jointly to the drag coefficient, it enters in the drag equation and is defined as the total area of the car and the device normal to the car direction.
- Drag area (C_d A) [m]: it is the product of the two previous terms (drag coefficient and frontal area) and it better translate into a single number the aerodynamic performance of the system, especially in comparing different cases.
- Pressure drop (Δp)[Pa]: it is the pressure difference across the filtering media inlet and outlet surfaces. It indirectly affects the capturing performance of the filtering media.
- Air flow rate ($\dot{V}$)[m^2/h]: it is the measure of the volume of air entering the device per unit of time.

Because of the 2D simplification the extensive quantities, as the Air Flow rate and the Frontal and Drag area, do not reflect the real units: they appear as specific quantities, namely divided by length units.

Lower drag coefficient and frontal area, likewise higher flow rate and pressure drop have to large extent to preferred and pursued in the study. Being these parameters strictly related, as shown in the equations previously presented, an overall perfect solution does not exist, and a balance has to be found. The simulation software used is COMSOL Multiphysics v5.3a, while the CAD software is Autodesk Fusion 360.

Davide Carlucci

4.1 Physical parameters

The first main issue in solving the state equations consists in the lack of some physical data regarding the material used. A preliminary step based on a literature review, with the aim to estimate the parameters of the filtering media necessary in the computation, is needed. Focus is put in the porosity and permeability.

The porosity (ε_p) is defined as the ratio between the void volume (V_{void}) and the total volume (V_{total}) of the material, hence a dimensionless parameter:

$$\varepsilon_p = \frac{V_{void}}{V_{total}}$$

It can be also calculated as the product of the pore volume and the apparent density of the material.

The permeability (k) expresses the capability of a material to let fluids pass through it and is measured in m^2.

Manufacturers usually do not provide the above-mentioned parameters (k and ε_p) for activated carbon, Methylene blue or Iodine value are more common but also vaguer and more inconsistent, so they are taken from literature. For Granular Activated Carbon it has been taken as reference a value of 0.49 for the porosity [21] and $4.69*10^{-9}$ m^2 for the permeability [22].

4.2 COMSOL Multiphysics interfaces

The simulation software used for the device CFD study is COMSOL Multiphysics v5.3a. Even without being the most used software for Computational Fluid Dynamics, it is very powerful when it comes to couple different physical systems with different, tough compatible, governing equations. Its intuitive interface and workflow are an advantage while performing parametric simulations.

The two physics used in the model are:

- ≈ **Turbulent Flow, k-ε** (spf): this interface is used for simulating single-phase flows at high Reynolds numbers. The physics interface is suitable for incompressible flows, and compressible flows at low Mach number (typically less than 0.3). The equations solved by the Turbulent Flow, k-ε interface are the Navier-Stokes equations for conservation of momentum and the continuity equation for conservation of mass. Turbulence effects are modeled using the standard two-equation k-ε model with realizability constraints. Flow close to walls is modeled using wall functions.

- 📘 **Free and Porous Media Flow** (fp): it is used to compute fluid velocity and pressure fields of single-phase flow where free flow is connected to porous media. The physics interface is well suited for transitions between flow in porous media, governed by the Brinkman equations, and flow in channels described by the Navier-Stokes equations. Fluids with varying density can be included at Mach numbers below 0.3. Also the viscosity of a fluid can vary, for example, to describe non-Newtonian fluids.

Davide Carlucci

4.3 Main assumptions in the simulations

To simplify the simulation process, some assumptions are made either on physical parameters, as above, or on the physics involved.

In this section all the assumptions made are briefly listed.

- The system, at this step, is considered 2D in the CFD studies. This is mainly done for computational cost purposes; in this way it is possible to do more simulations in less time without having big compromises in term of mesh resolution and solution accuracy. In fact, even being known that the 2D CFD simulation leads to an imprecise determination of the drag forces acting on the car, the main aim of this study is to compare between each other the performances in every case.

- Being the simulations 2D, the device is thus considered of the same width of the car even if it is not like; the lateral airflow is ignored leading to a probable overestimation of the drag induced, that is still preferable than an underestimation in order to avoid the effectiveness of the device. More realistic results will be obtained in the 3D simulations, which are treated in detail in the Chapter 5.

- In the 3D simulations, the filtering media area has an arbitrary value, chosen to give the device an easy manageability by one person.

- Only stationary conditions are considered, in which the car speed is constant. Higher solicitations have to be expected, under real operating condition, due to car accelerations and cross winds.

Davide Carlucci

4.4 Reference case: 2D car simulation

To study the behavior of the system it is necessary to study it into real operating conditions, so while being mounted on the car. Prior to this, a CFD study of the car alone is needed, to compare it with the further analysis with the device on place. The simulations will be held at different speed with the aim to evaluate the drag coefficient, the area and so the drag area of the car.

Figure 16 Volkswagen Golf V is the model of car studied [23]

As reference case for the simulations the Volkswagen Golf V car model is chosen (Figure 16) [23]. This choice is due to its very wide spread in the European market, ranking 1st in sales [24] in 2018, and in the Spanish one as well, being the 3rd most sold car in Spain [25] in the same year.

4.4.1 Car CAD repair

Since the study is 2D, for the reasons mentioned, only the silhouette of the car is used.
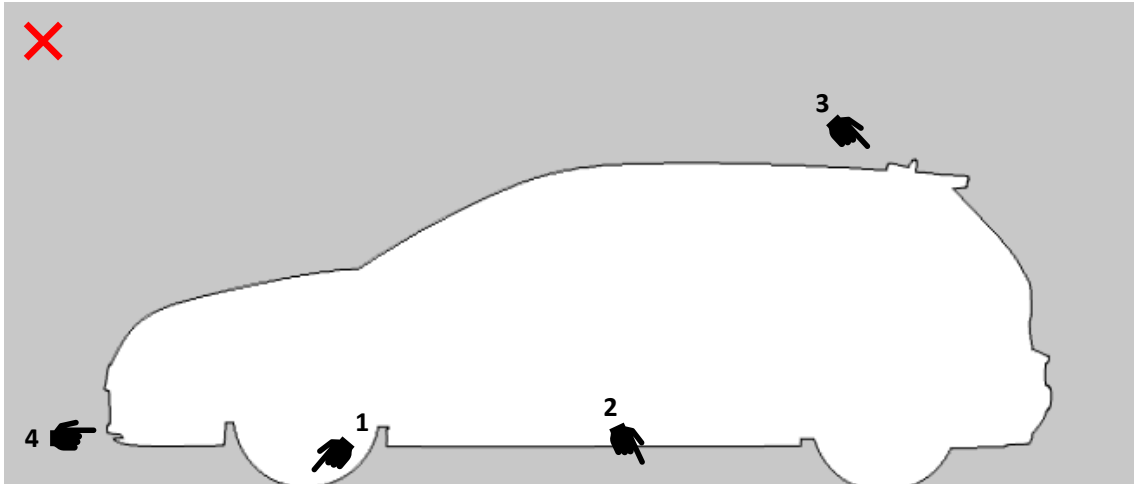

Figure 17 2D car silhouette CAD before repairing
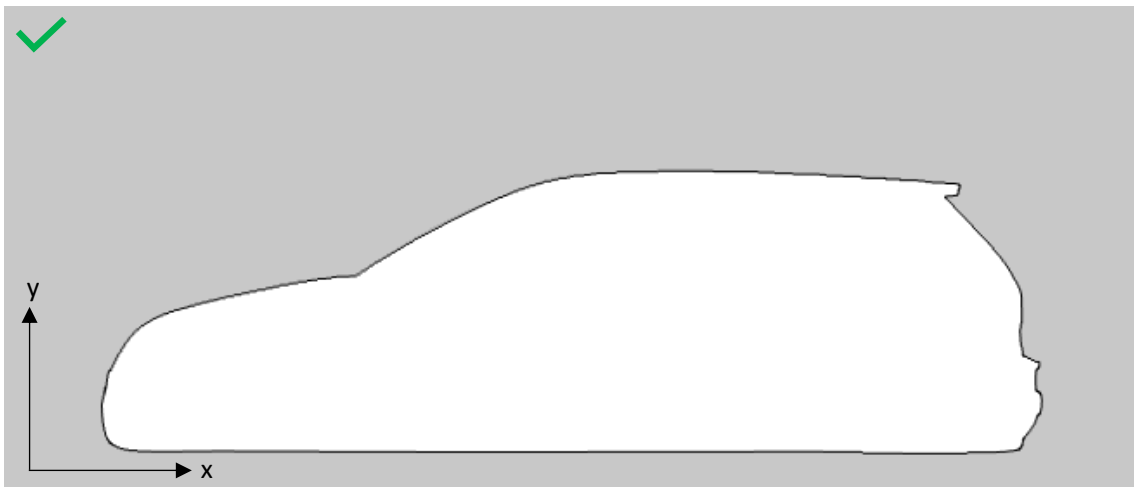
Figure 18 2D car silhouette CAD after repairing

While computing an automotive 2D CFD study it is important to remove the wheels from the body (Figure 17), because they generate an unreal stagnation point (point 1), and a resultant low speed zone, in the proximity of their front part that causes a huge distortion from the reality. This also origins a separated gap (point 2) in which the air is still: a situation that is far from the real case and common sense. Moreover, some adjustment are made on the drawing, like removing the radio antenna (point 3) and the front lights appendices (point 4), to generate an easier CAD (Figure 18) and simplify the computation.

4.4.2 Simulation setup

Only the Turbulent Flow interface is used, due to the absence of the device. The domain needed for the computation has to be wide enough to contain the vehicle itself and let a relaxation of the computed dependent variables.

Figure 19 Domain dimensions for the 2D simulations

Thus as rule of thumb the domain considered has three times the length of the car behind it, one in front and one height on it, appearing like in Figure 19.

The following constraints are applied for Turbulent Flow physics (spf):

- Boundary 1: Inlet - Normal inflow velocity (range(10,10,80) [km/h])
- Boundary 2: Outlet – Pressure (0 [Pa])
- Boundary 3: Open Boundary – Normal stress (0 [N/m^2])
- Boundary 4: Wall – Wall condition (no slip)
- Boundary 5: Wall – Wall condition (no slip)
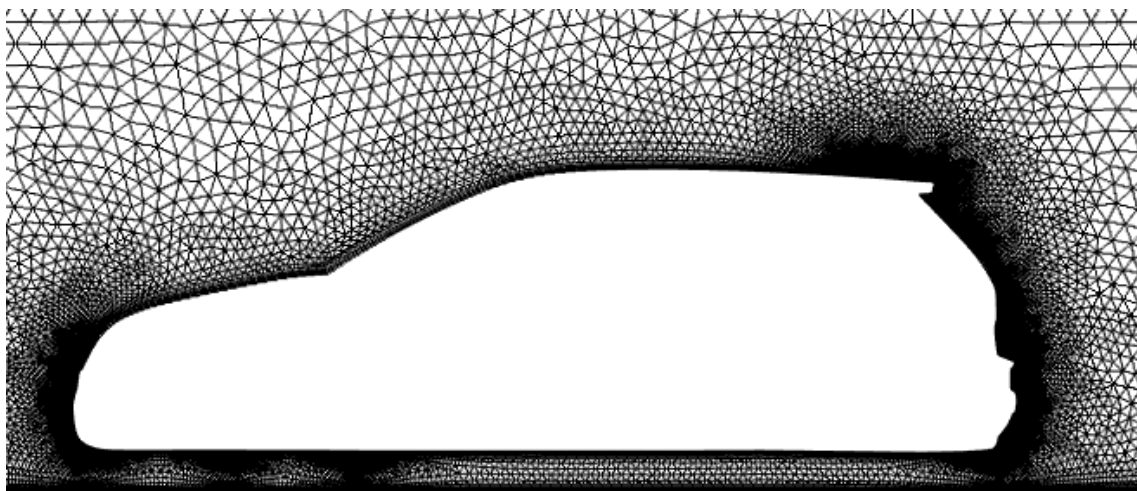
Figure 20 Domain mesh around the car body

Davide Carlucci

Being the reference case for all the further simulations, a *Fine* physics-controlled mesh is used (Figure 20), for more accurate results. With the chosen mesh the number of elements generated is 106,706.
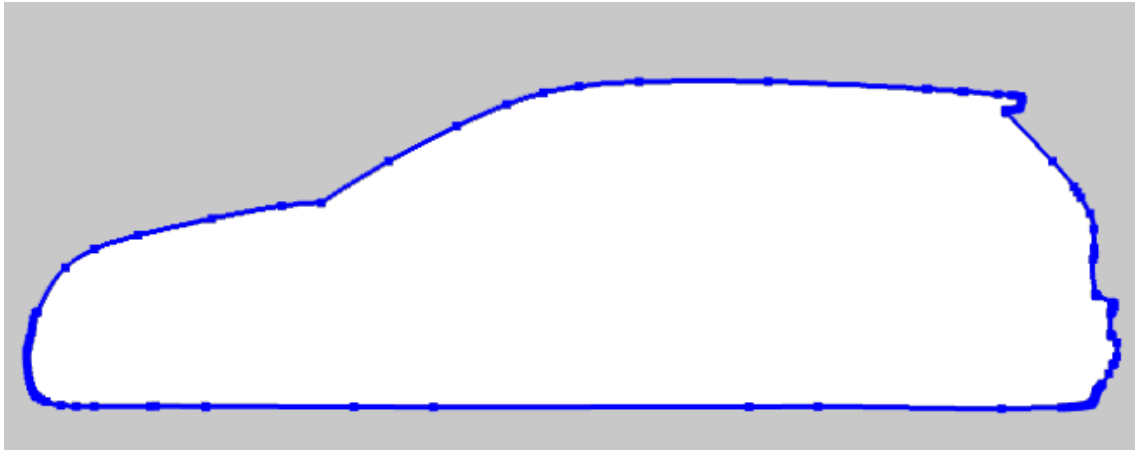

Figure 21 Boundary selection for drag coefficient *global evaluation* (car)

The Drag coefficient is computed through *global evaluation* as follows:

$$C_d = -2*intop1(spf.T\_stressx)/(aveop1(spf.rho)*(speed^2)* intop1(nx*(nx>0)))$$

Where:

- *intop1(spf.T_stressx)* is the integration along the car shape (Figure 21) of the x-component of total stress;
- *aveop1(spf.rho)* is the density of the air;
- *speed* is the speed at the inlet boundary;
- intop1(nx*(nx>0)) is the car frontal area (A) calculated as integration along the car shape of the positive x-normal vectors at the boundary.

Davide Carlucci

4.4.3 2D reference case results

The simulation converges after *6h 28m 9s*. The plot of the drag coefficient at different speed is presented (Figure 22):


Drag coefficient - reference case
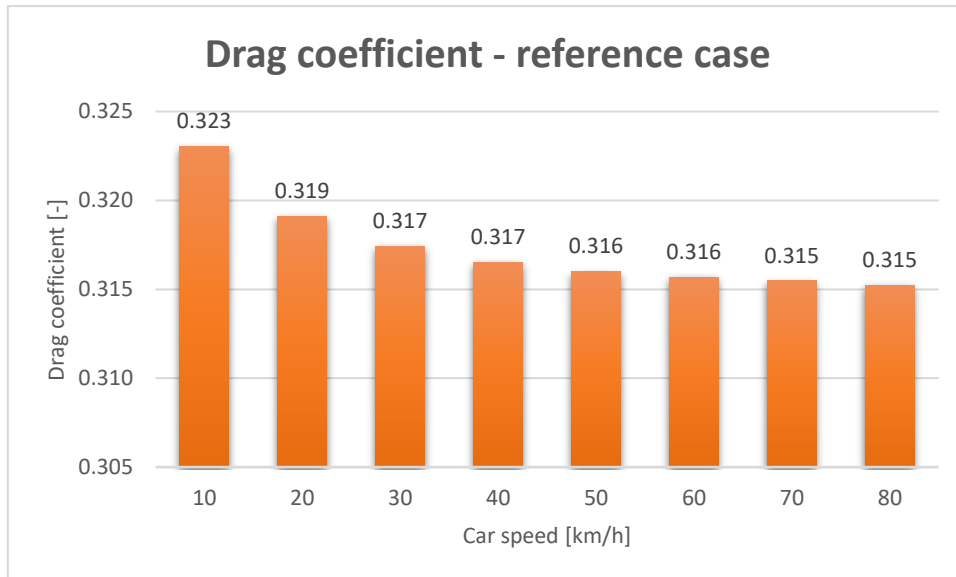
Figure 22 Drag coefficient variation at different speeds

The C_d, as previously said, is speed-dependent and slightly decreases with the speed.

Table 3 Main indicators for the 2D reference case (only car)

2D Reference case

C_d	0.315
A	1.344 m
C_dA	0.423 m

As reference overall value it is taken the one at 80km/h that is equal to 0.315 (Table 3). The frontal area, calculated in meters because of the 2D simplification, is 1.344 m. Thus, the multiplication between the two factors (C_dA) becomes 0.423 m.

Davide Carlucci

The Volkswagen Golf real drag coefficient is estimated to be around 0.35 [26], implying an error in the simulation of 11% mainly due to the 2D simplification. This error, even seeming big, is considered acceptable in the CFD analysis.
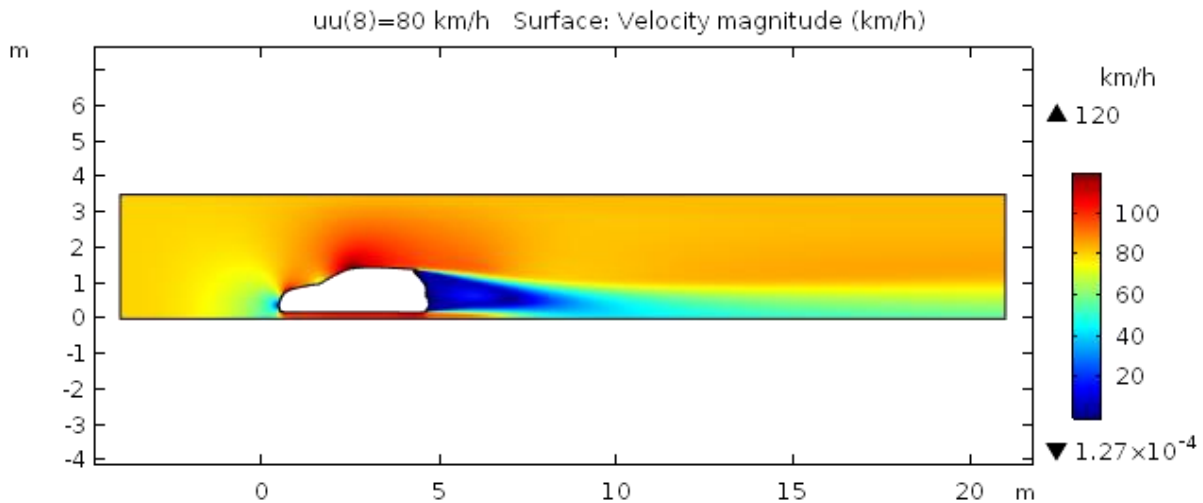

Figure 23 Velocity magnitude field at car speed of 80 km/h
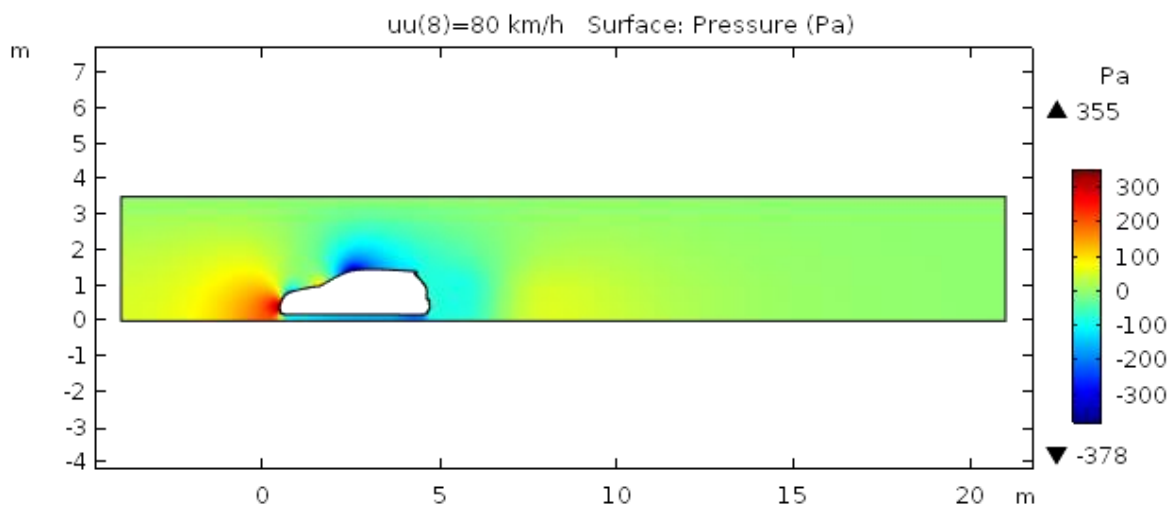
Figure 24 Pressure field at car speed of 80 km/h

The velocity magnitude (Figure 23) and the pressure (Figure 24) at 80km/h of speed are reported. It is easy to recognise the stagnation point, in which the velocity is zero and the pressure is maximum, in the front of the car and the low-pressure zone at the beginning of the roof.

4.5   Device design and CAD

While designing the shape of the device, it has been taken inspiration from the roof scoops (or roof vent) and hood scoops (hood vent) of the race car, in particular the rally ones.

Figure 25 Roof scoop used in rally cars [27]

The purpose of roof scoop (Figure 25) [27] is to pressurize the cabin, by pushing air in it, to avoid the dust from entering and disturbing the view of the driver. Because of its scope, the vent has to be placed in the part of the roof closest to the windshield; this constraint is not present in our application, giving so more freedom in the device placement above the roof surface.

Davide Carlucci

Figure 26 Hood scoop used in rally cars [28]

The hood scoop (Figure 26) [28] is used to cool the engine, instead, so its position is determined by the location of the engine itself inside the front compartment.

Being both custom solutions used in motorsport, the scoop profile adapts to the car shape. This is not possible for the design of our device since it is supposed to be universal and adaptable to every car. Besides that, the scoops are always permanent and not removable
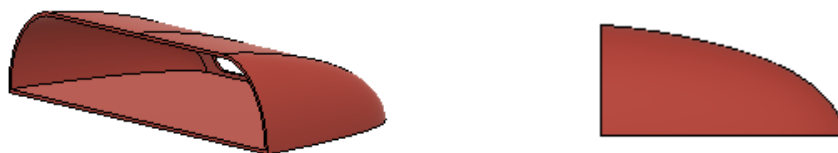
Figure 27 Device CAD (version 1) general view (left) and lateral view (right)

Starting from this idea the first CAD model of the device has been drawn (Figure 27). A simple shape is chosen at this step to avoid complications in the simulation and have lower approximation error to the 2D simplification. In fact, since only the cross section is taken into account, it is better to avoid more complex shape at this step, being the lateral airflow neglected.
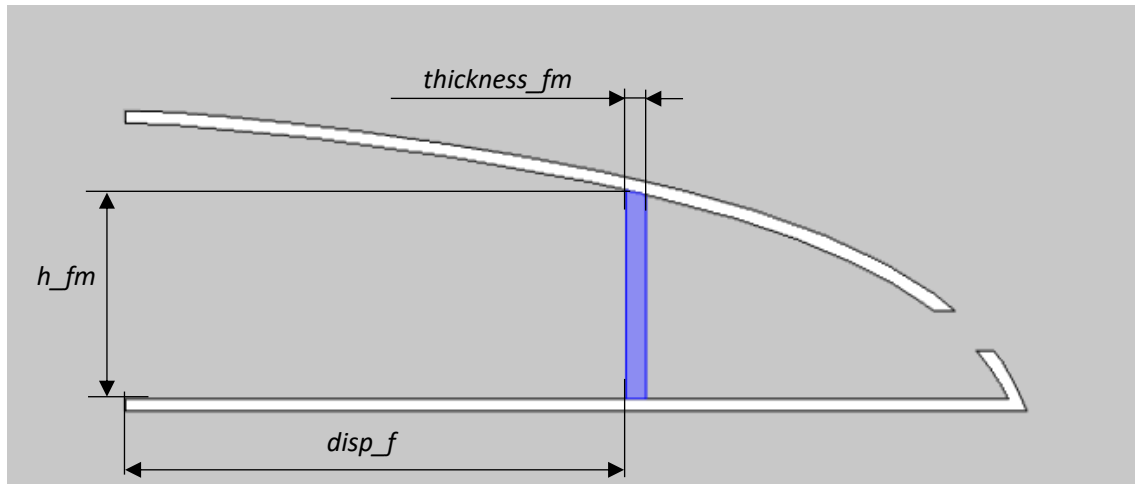

Figure 28 Device 2D cross section (version 1)

Then its 2D maximum cross section (Figure 28) has been imported in COMSOL to be studied.

The filtering media is added later in COMSOL with the following arbitrary initial parameters:

- *thickness_fm*: it is the thickness of the filtering media (10 [mm]). This value has been chosen because of the filtering media average size that is of the same order of magnitude;
- *disp_fm*: it is the distance between the inlet of the device and the filtering media (25 [cm]).

At this value of *disp_fm* the precise height of the filtering media (*h_fm*) is 10.5 cm.

Davide Carlucci

4.6 System 2D simulation

The simulation on the system, considered as car plus device, implies the solution of two different physics: *Turbulent Flow* (for the car and device frame) and *Free and Porous Media Flow* (for the filtering media). At the interface between the two domains with different physics the proper coupled constraints have to be set. Two different mounting positions have been investigated: on the roof (*case A*) and on the hood (*case B*). Within the *case A*, further different position adjustments are discussed, thanks to the degrees of freedom that this position gives. In fact, while mounting the device on the hood, it has to affect the visibility of the driver as less as possible and so it can be installed only directly connected to the hood itself.

4.6.1 Device case A: x-position parametric analysis

The following simulations investigate the proper device position on the car roof along the x axis.
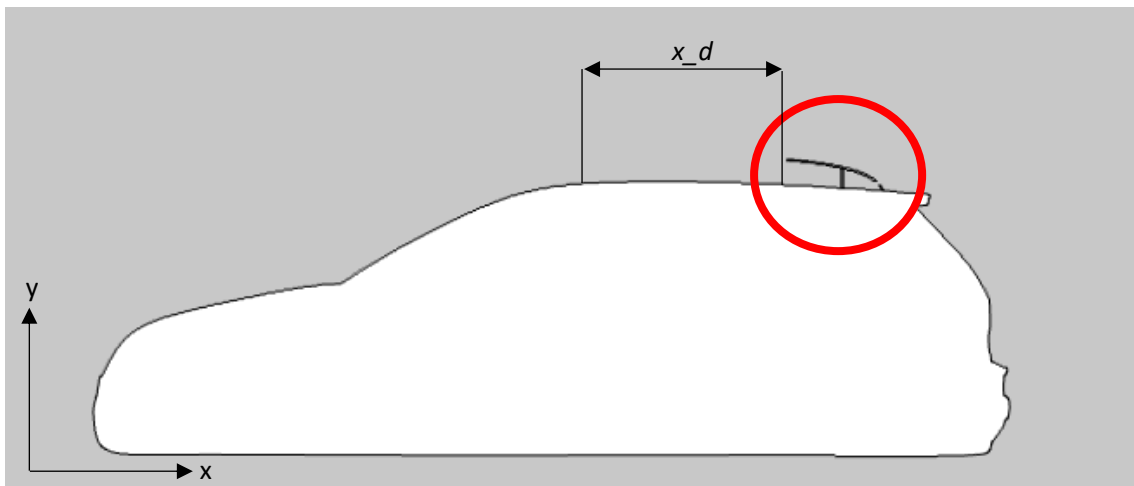
Figure 29 Device relative distance to the roof beginning along the x-axis

The length x_d represents the distance between the beginning of the roof and the inlet of the device (Figure 29).

For the *Turbulent Flow* (spf2) the same boundary conditions as the previous study are applied. For the Free and *Porous Media Flow* (fp), shown in Figure 30, the settings are:

- Boundary 6: Inlet – Velocity field (u_0=(spf2.u2,spf2.v2) [m/s])
- Boundary 7: Outlet – Pressure (spf2.p2 [Pa])
- Boundary 8: Wall – Wall condition (no slip)
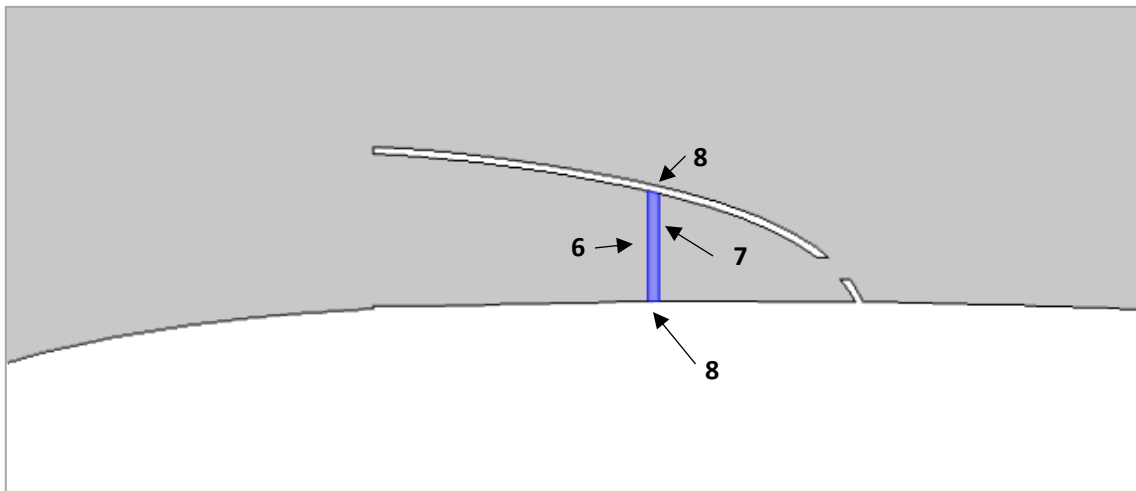
Figure 30 Filtering media boundaries shown

Different speeds are simulated; the boundary conditions and the *parametric sweep* input are:

- Boundary 1: Inlet - Normal inflow velocity ((30,50,80) [km/h])
- *x_d* parametric sweep: (range(0,30,90) [cm])

An *Extremely Coarse* physics-controlled mesh is used and the simulations converge in *1h 29m 24s*.
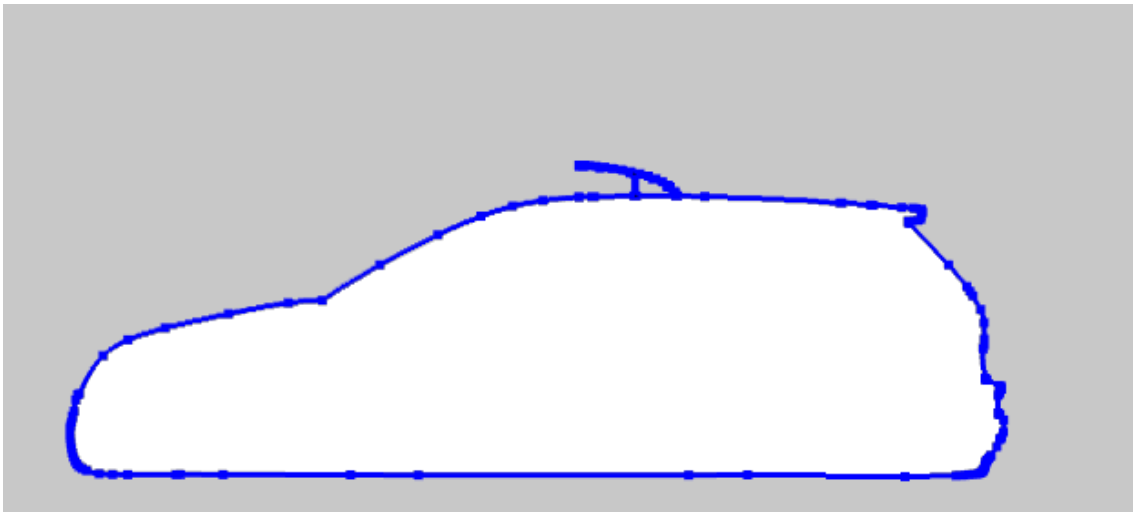
Figure 31 Boundary selection for drag coefficient *global evaluation* (car + device)

The Drag Coefficient C_d is calculated as before but the integration boundary changes because of the presence of the device (Figure 31), which has to be taken into account.

The Pressure Drop Δp across the porous media is computed through *global evaluation* as follows:

$$(8.5) \quad \Delta p = \text{aveop2(p2)-aveop3(p2)}$$

where

- *aveop2(p2)* is the average pressure at the porous media inlet (6 in figure);
- *aveop3(p2)* is the average pressure at the porous media outlet (7 in figure).

The Air Flow Rate $\dot{V}$ crossing the porous media is computed through *global evaluation* as follows:

$$(8.5) \quad \dot{V} = \text{-aveop2(spf2.U)*intop2(nx*(nx<0))}$$

where

- *aveop2(spf2.U)* is the average velocity magnitude at the porous media inlet (6 in figure);
- *intop2(nx*(nx>0))* is the integration along the porous media inlet of the positive x-normal vectors at the boundary (6 in figure).

Davide Carlucci
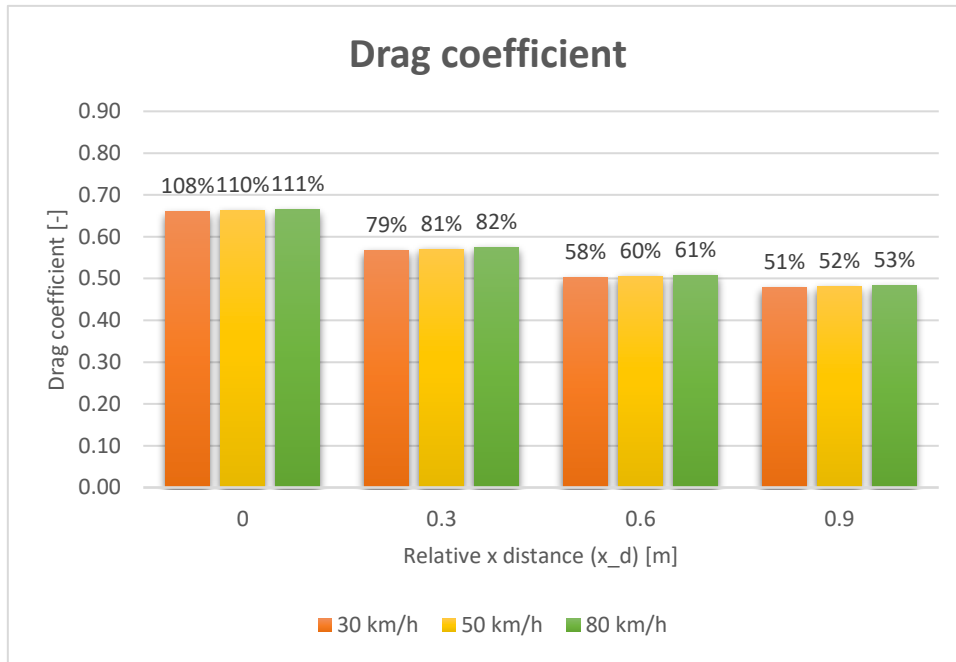
Figure 33 Drag coefficient at different relative x distance and car speed

In the Figure 33 is clearly visible that at the maximum relative distance (*x_d*=90 cm) the overall drag coefficient reaches the lowest value (C_d=0.482 at *x_d=0.9 m* vs C_d=0.664 at *x_d=0* m). The percentage values represent the increment in respect to the reference case. It emerges that the drag coefficient values are slightly speed dependent, though showing very little difference between each other at given device position.
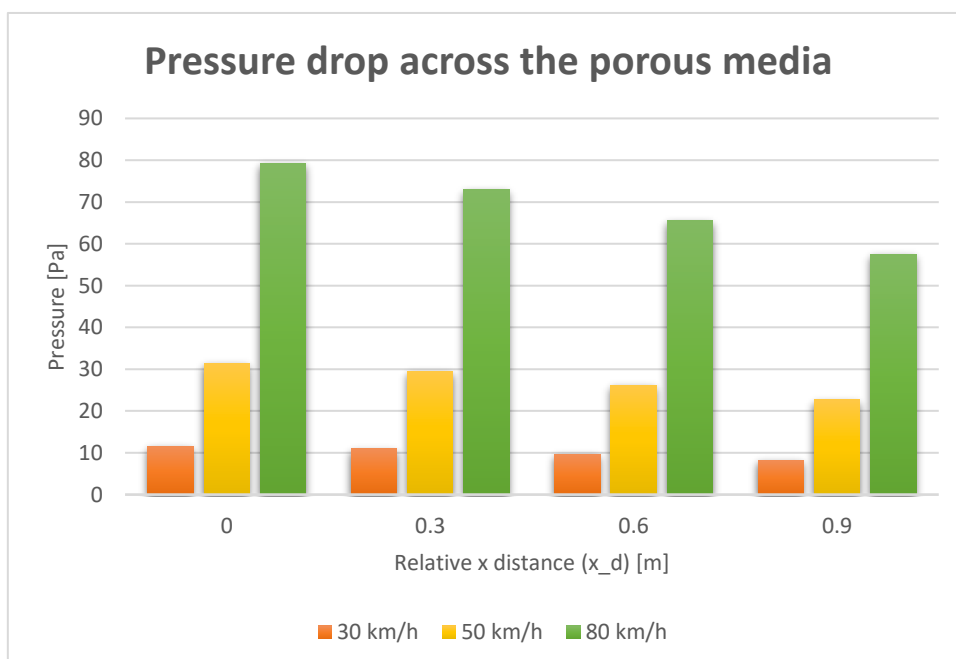

Figure 32 Pressure drop across the filtering media at different relative x distance and car speed

The drawback is, that also the pressure drop (Figure 32) and the flow rate (Figure 34) decrease, but with a slower trend. Their speed dependence is high if compared to what the drag coefficient showed.
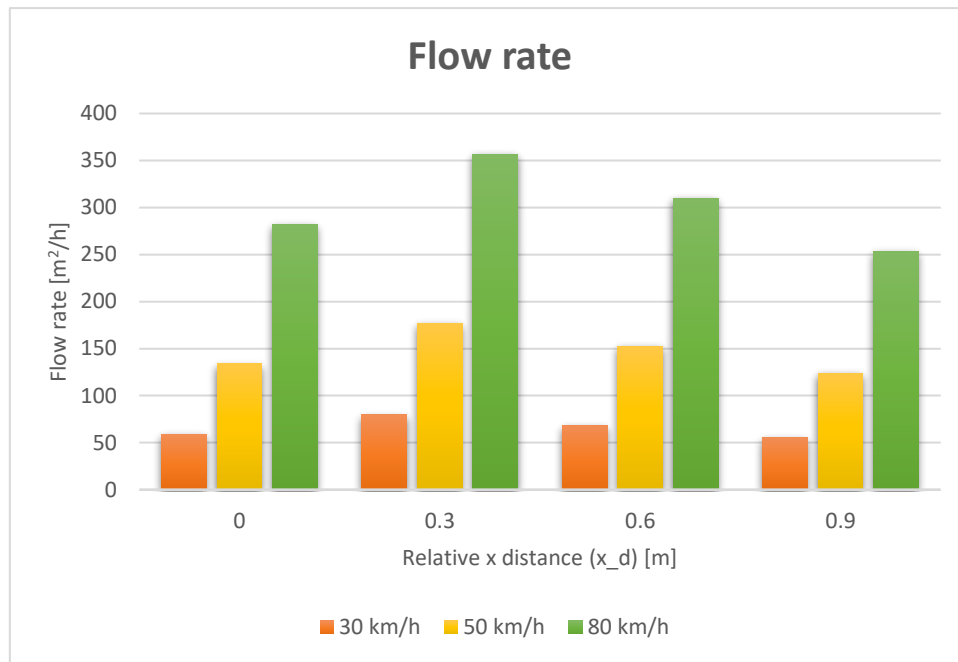

Figure 34 Flow rate across the filtering media at different relative x distance and car speed

The air flow rate through the device has a non-monotonic behaviour: it increases reaching a maximum for x_d=0.3 and then decreases (Figure 34). For both the pressure drop and the flow rate, the lowest value is never more than 30% less than the maximum value. This justifies the main importance given to the drag coefficient that can easily vary in a wider range.

Davide Carlucci
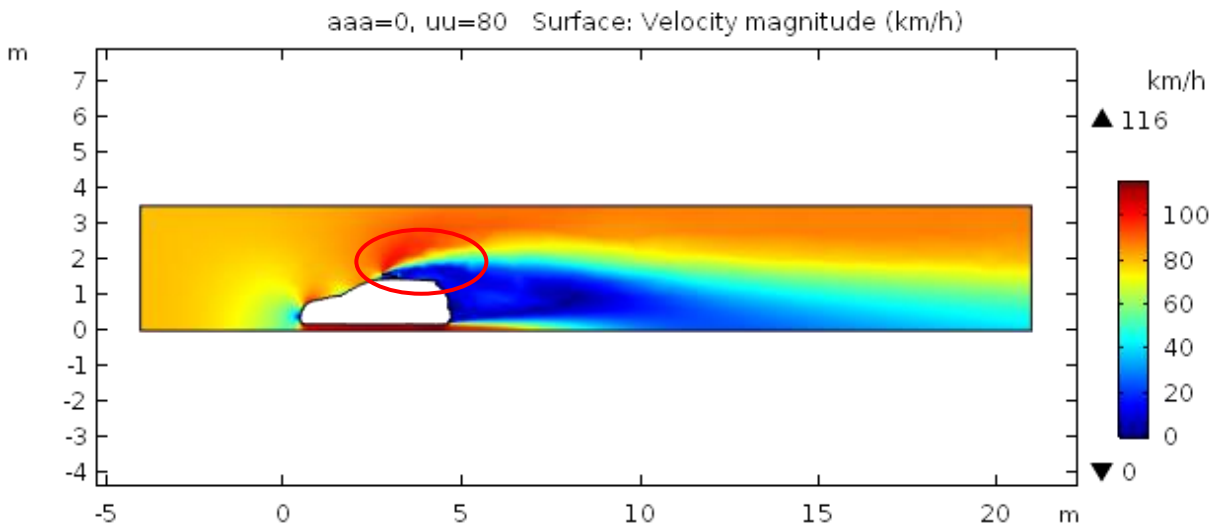
Figure 35 Velocity magnitude field at car speed of 80 km/h and device mounted (x_d=0 m)
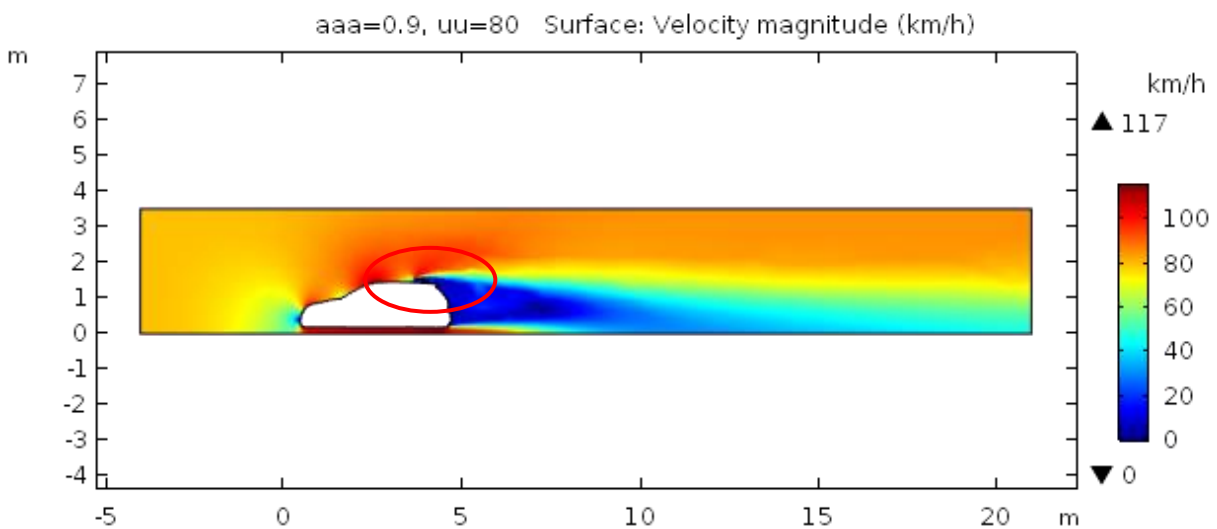
Figure 36 Velocity magnitude field at car speed of 80 km/h and device mounted (x_d=0.9 m)

It is useful to visually compare the velocity magnitude plots at the minimum (Figure 35) and maximum value of x_d (Figure 36). In this way it is extremely intuitive to understand why the backward position gives better results in terms of drag: the wake zone behind the car is much smaller and closer to the case of the reference case.

Davide Carlucci
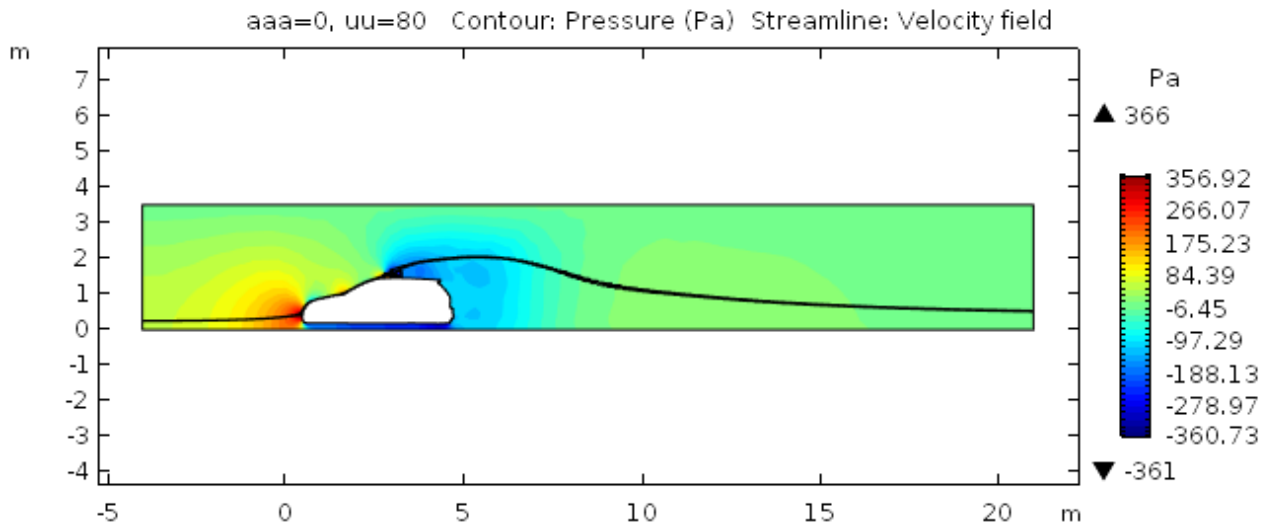
Figure 37 Pressure field and streamlines crossing the device at car speed of 80 km/h and device mounted (x_d=0 m)
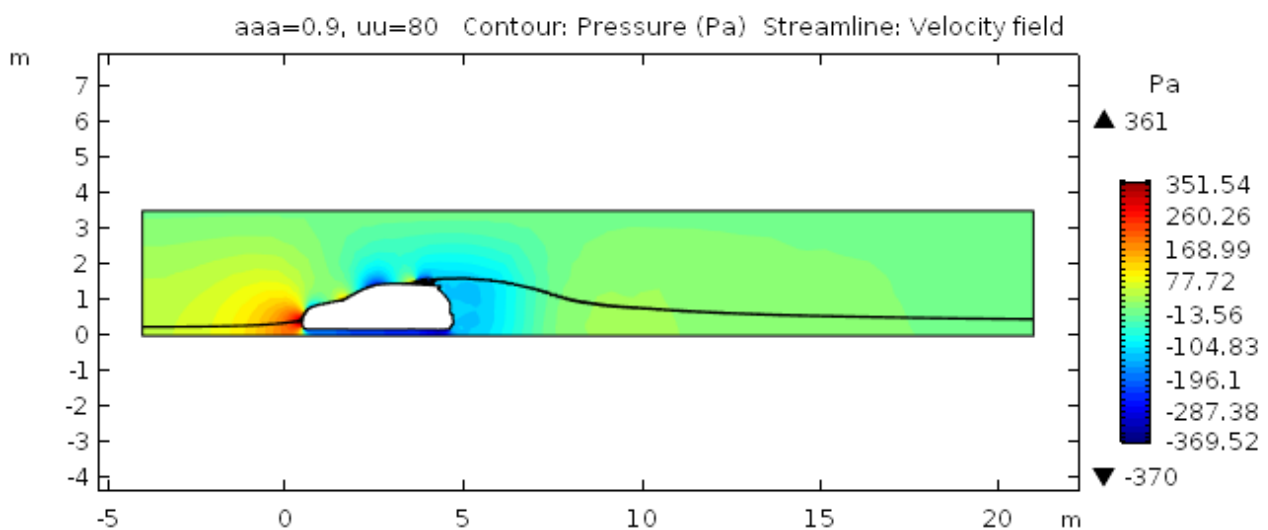
Figure 38 Pressure field and streamlines crossing the device at car speed of 80 km/h and device mounted (x_d=0.9 m)

How the two positions affect the performance of the car is seen also through the pressure plots, being the pressure and the velocity related. The low pressure zone past the device, while mounted in frontmost position (Figure 37**Error! Reference source not found.**), is bigger than the latter case (Figure 378). The streamlines (black lines in figure) crossing the filtering media inlet (boundary 6) are confirming this aspect: the more

frontward the device is placed, the higher the streamlines go past the device enhancing the aerodynamic resistance.

Davide Carlucci
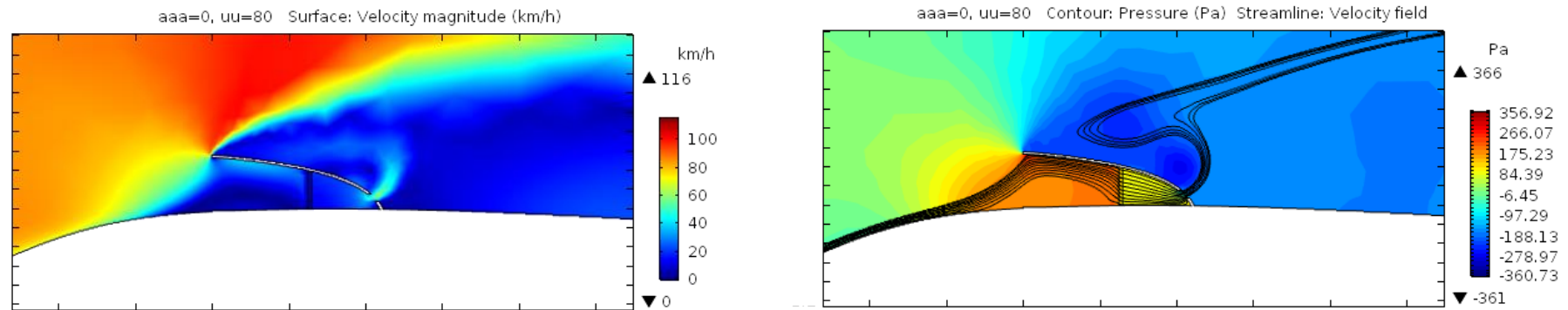
Figure 39 Velocity magnitude (left) and Pressure field and streamlines crossing the device (right) at car speed of 80 km/h and device mounted (x_d=0 m)
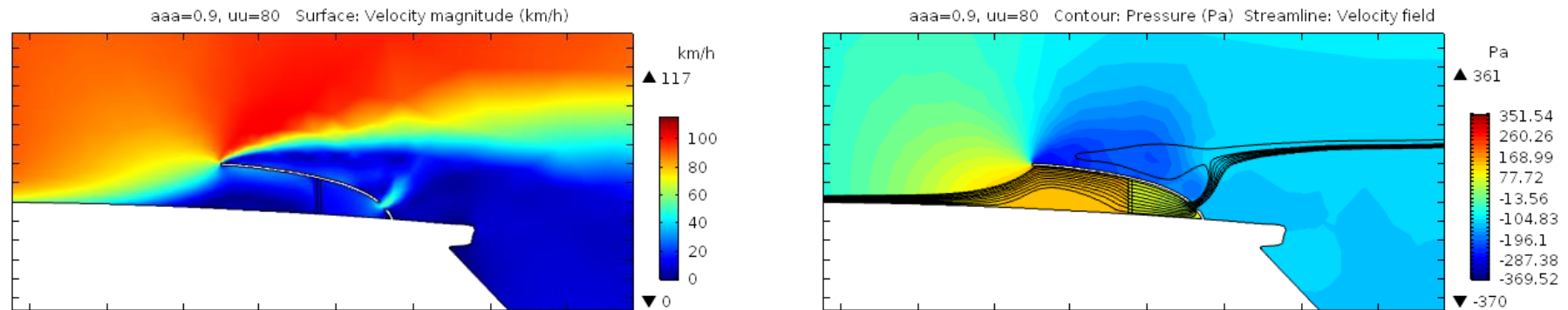

Figure 40 Velocity magnitude (left) and Pressure field and streamlines crossing the device (right) at car speed of 80 km/h and device mounted (x_d=0.9 m)

Local pressure and velocity at device scale are reported (Figure 39 and Figure 40) for the two extreme cases.

Davide Carlucci

4.6.2 Device case A: y-position parametric analysis

The following simulations investigate the proper device position on the car roof along the y axis.
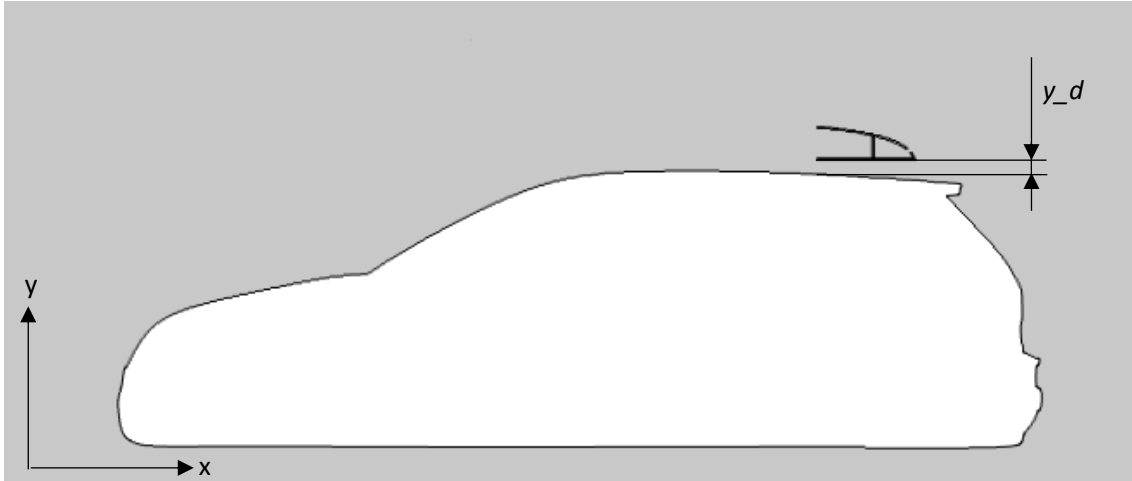

Figure 41 Device relative distance to the roof along the y-axis

The length y_d represents the distance between the bottom part of the device and the car roof closest point (Figure 41).

The boundary conditions are set as before except for the inlet speed. In fact, after the previous simulations results, it has been decided to carry simulations only at 80 km/h because this is the most delicate case and generates the worst results in terms of performance for all the indicators.

The new boundary conditions and *parametric sweep* inputs are:

- Boundary 1: Inlet - Normal inflow velocity (80 [km/h])
- *x_d* parametric sweep: (range(0,30,90) [cm])
- *y_d* parametric sweep: (range(5,5,10) [cm])

An *Extremely Coarse* physics-controlled mesh is used and the simulations converge in *1h 1min 22s*.

Davide Carlucci
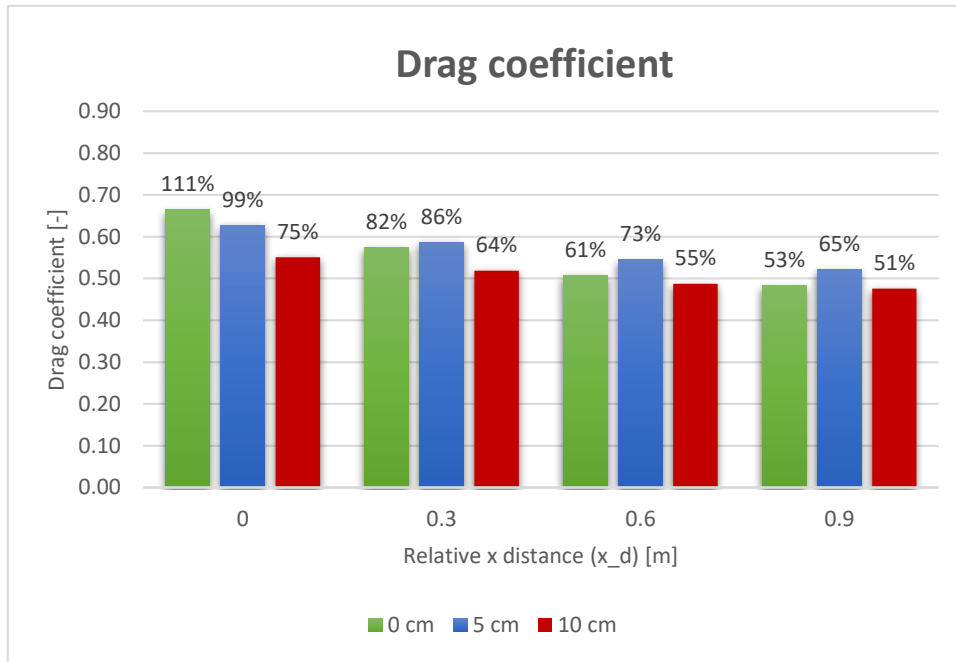
Figure 42 Drag coefficient at different relative x-y distance combination

The drag coefficient trend is not monotonous at increasing values of *y_d* (Figure 42), having high peaks at intermediate values of elevation (*y_d*=5 cm). Evaluating the overall performance, it comes that the best elevation is *y_d*=10 cm.
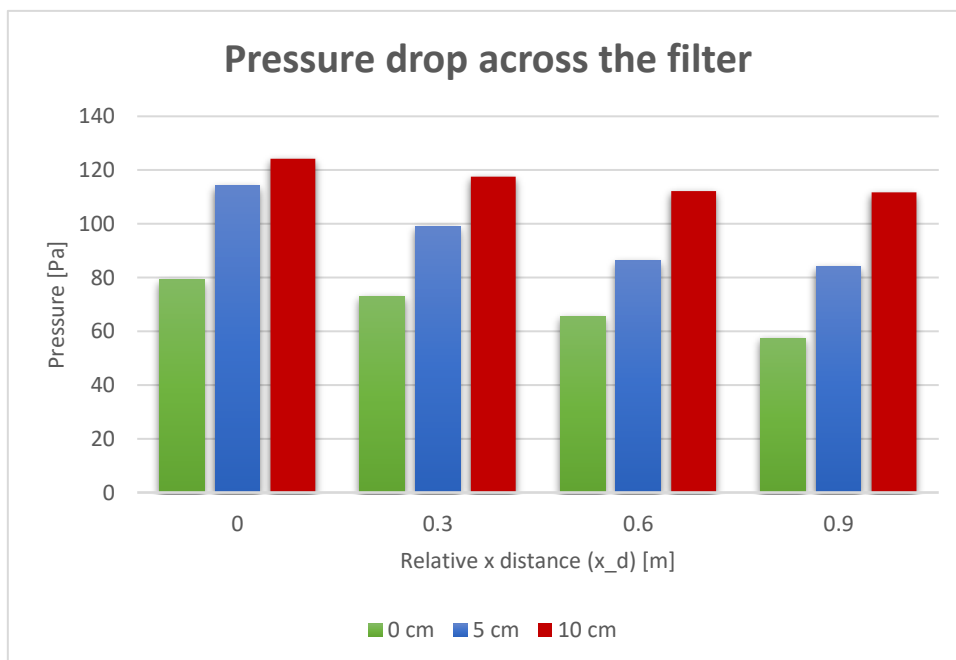
Figure 43 Pressure drop across the filtering media at different relative x-y distance combination

Davide Carlucci

At the highest elevation the drag reduction is high in most of the cases, as well as the pressure drop (Figure 43), if compared to the values at $y\_d=0$.

This behaviour is caused by the too short distance between the device and the roof that does not let the air pass easily through it. In fact, in this small gap, the air flows at very low speed and there is only a side effect of an increase of the apparent frontal area of the device.
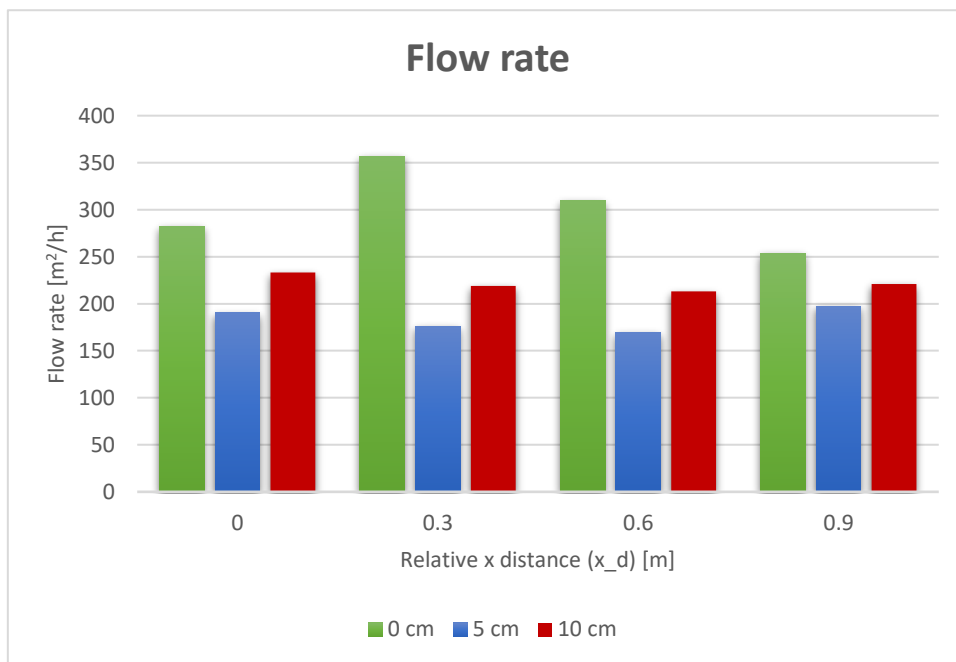
Figure 44 Flow rate across the filtering media at different relative x-y distance combination

Subsequently also the flow rate is penalised by this effect (Figure 44), while the pressure drop appears enhanced instead.

Davide Carlucci

The above-mentioned behaviour is easier detected looking at the velocity magnitude field.
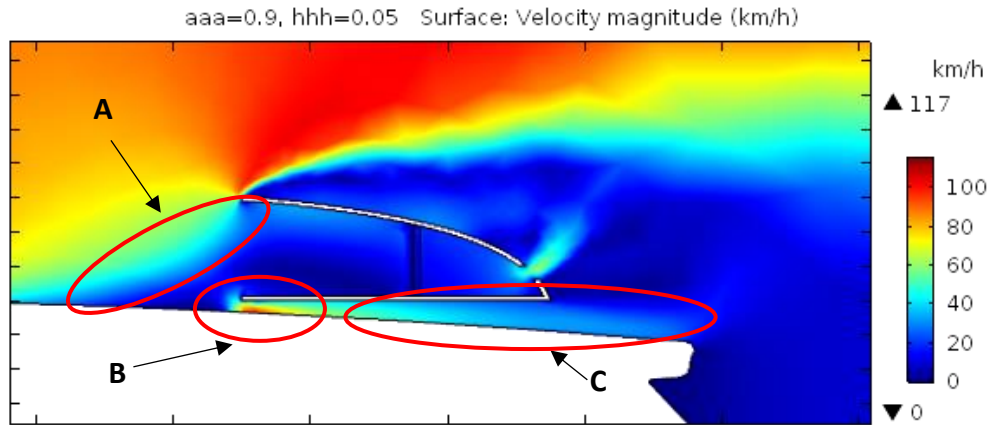
Figure 45 Velocity magnitude field at car speed of 80 km/h and device mounted
(x_d=0.9 m / y_d=0.05 m)
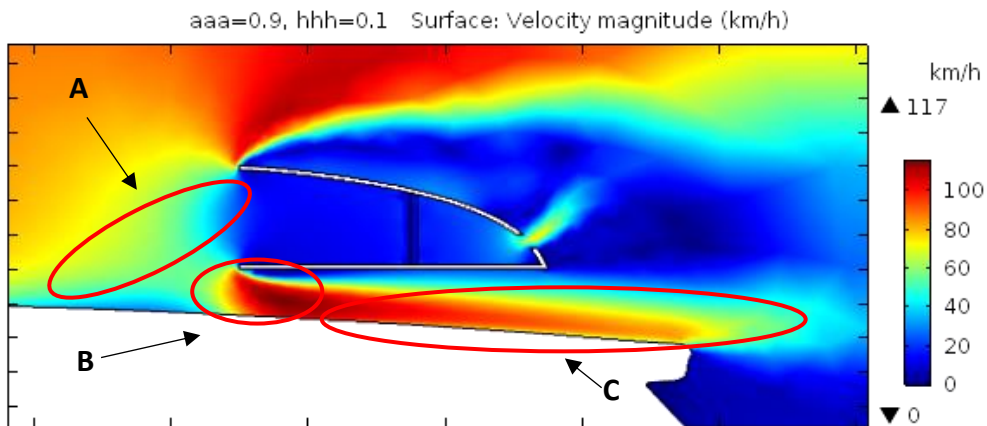
Figure 46 Velocity magnitude field at car speed of 80 km/h and device mounted
(x_d=0.9 m / y_d=0.10 m)

The highlighted zones A (Figure 45 and Figure 46) are the prove of the better performances developed by a bigger y_d value: in fact, at y_d=0.05 m, the air flow under the device is still obstructed by the too thin gap. At y_d=0.10 m gap is sufficient to let the air pass through at high speed (zones C)

Davide Carlucci

From the same figures(Figure 45 and Figure 46), it is visible also how the shape of the device affects the airflow around it (zones B): the bottom part of the device has been designed as a plane, because of the initial mounting position idea (directly on the roof). In this position, and in general at non-zero elevation of the device, changes in the bottom shape could lead to further drag reduction.

4.6.3 Conclusion on case A

In the first of the two mounting positions proposed (on the roof), after studying various combinations of (x_d, y_d), it is clear that the combination that gives the lowest drag is (0.9 [m], 0.1 [m]). This means that the furthest the device is from the roof beginning the more an early detachment of the flow occurs. This basic principle can be applied also to other car versions. Then it has been understood that is preferable to place the device not in direct contact with the car, trying to leave a certain gap that has to be at least of around 10 cm.

Main indicators in the best case of case A are (Table 4):

Table 4 Main indicator for the Case A that showed the best performances (x_d=0.9 m / y_d=0.0 m)

Case A (best sub-case)	
C_d	0.476
A	1.508 m
C_dA	0.717 m
Δp	111.7 Pa
$\dot{V}$	221.1 m²/h

4.6.4 Device case B

The following simulations investigate the device performances while mounted on the car hood. Parametric study will not carried because of the constraints that this mounting position brings.

Figure 47 Device position on the car hood

An intermediate position on the hood is chosen to avoid obstaculation to the driver view but also to prevent the device to exceed the length of the hood cover itself (Figure 47). The device has the same shape and the boundary conditions are set as in the previous studies. Simulation are carried only at 80 km/h for its above mentioned criticality.

A *physics-controlled Extra Coarse* mesh is used and the simulation converges in *20min 55s*.

The results are processed, as usual, and the main indicators are extracted using the *global evaluation* tool. As frontal area it is taken the same value of the reference case being the device mountend in a position in which it does not affect the frontal area of the system.

Davide Carlucci

In this mounting position the main indicators are (Table 5):

Table 5 Main indicators for the Case B (hood mounting position)

Case B	
C_d	0.404
A	1.344 m
C_dA	0.543 m
Δp	129.9 Pa
$\dot{V}$	284.7 m²/h

These values are compared with the reference case and the case A case at its best performance (x_d=0.9 [m], y_d=0.1 [m]).
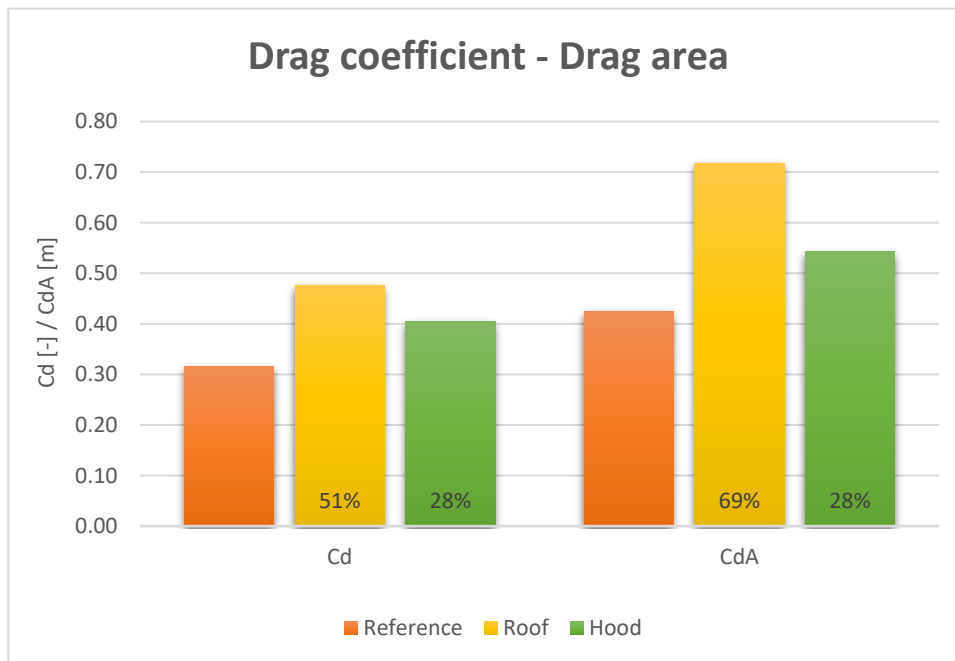
Figure 48 Drag coefficient and area comparison between the reference car and the two mounting position cases

The drag coefficient in case B is 0.404, 28% more than the reference case (Figure 48). Being the frontal area the same in the two cases also the drag area faces the same relative increment. This represents an improvement if compared to the best case in

Davide Carlucci

mounting postion1, that registered and increment of 51 % for the drag coefficient and 61% for the drag area.
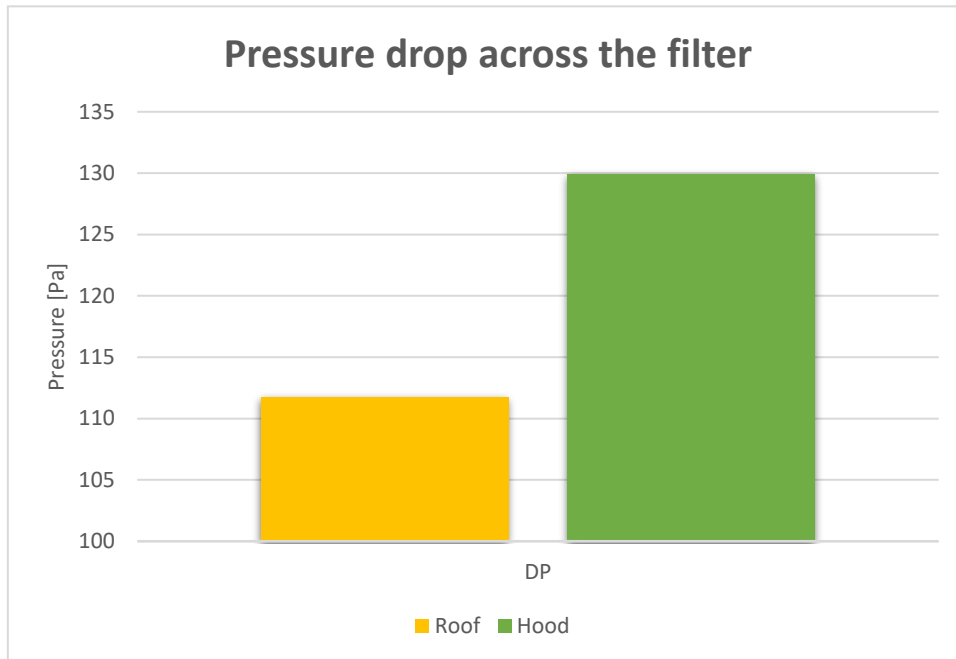
Figure 49 Pressure drop comparison between Case A and case B
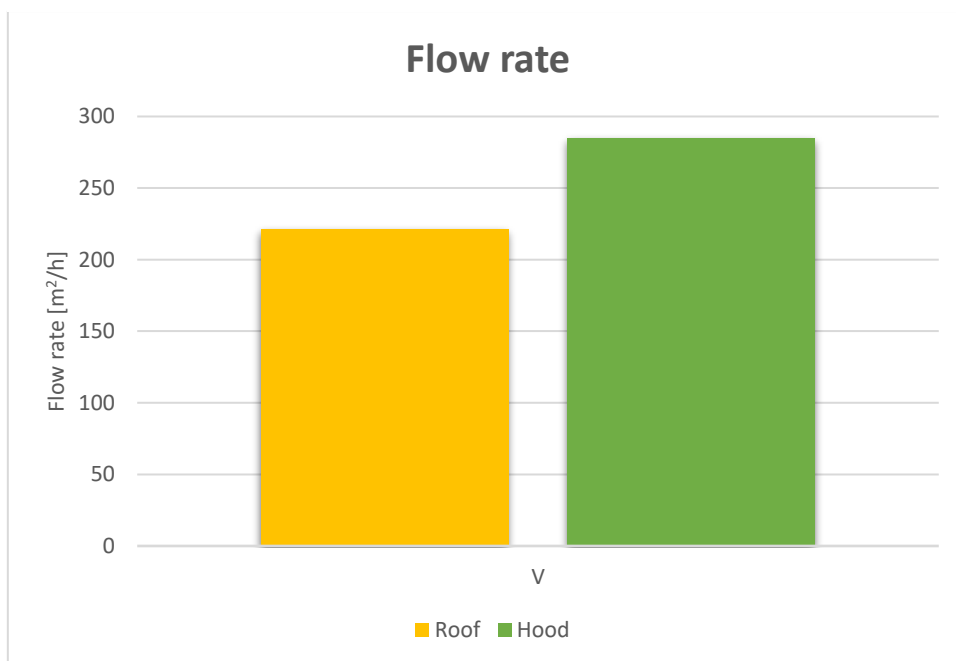
Figure 50 Air flow rate comparison between Case A and case B

The pressure drop slightly increases in hood position (129.9 Pa vs 111.7 Pa), being so the highest value between all the cases so far (Figure 49). The air flow rate increases as well (284.7 m²/h vs 221.1 m²/h) (Figure 50).

Davide Carlucci
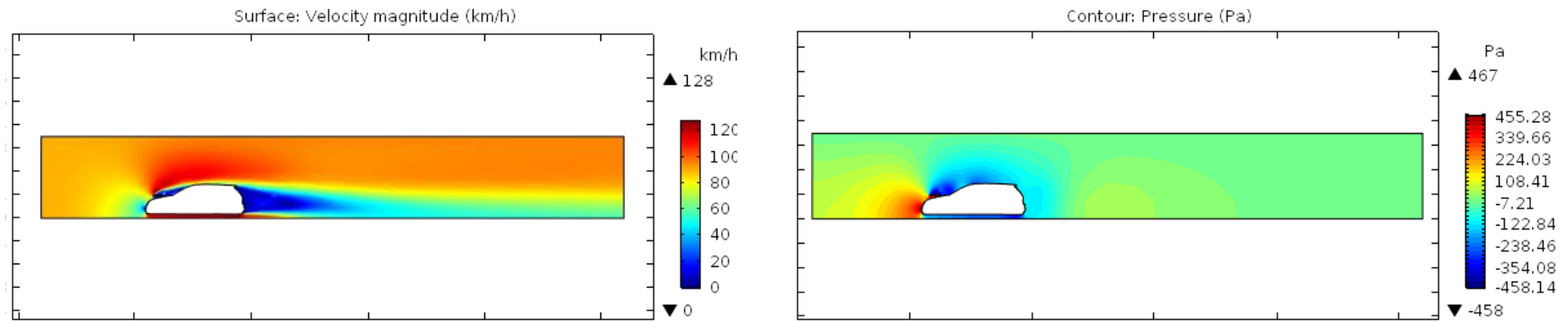
Figure 52 Global velocity magnitude field (left) and pressure field (right) for case B
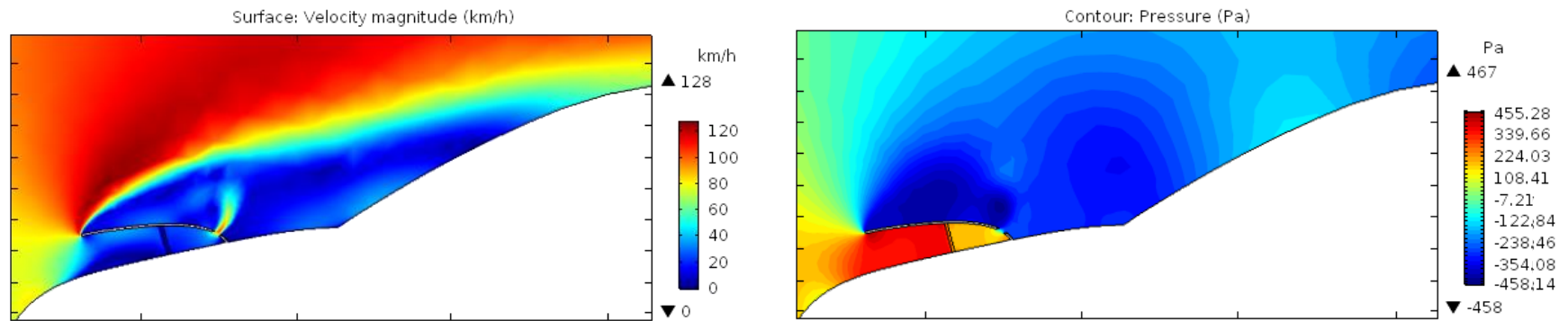
Figure 51 Local velocity magnitude field (left) and pressure field (right) for case B

Global and local pressure and velocity are reported (Figure 51 and Figure 52).

4.6.5   Conclusions on case B

Comparing the various mounting positions, it appears how it can significantly affect the overall system performance. In the case A, the best position is at the highest values of elevation and longitudinal distance, among the ones studied. The case B, because of the lack of degrees of freedom in the position, has been studied only once. Anyhow it shows better performance and it has to be preferred at the case A, when possible. In fact, some cars hood shape is more suitable than others to hold the device on itself without compromising the driver view.

4.7   Flow analysis and device shape optimization

After performing simulations placing the device in different parts of the car, all the data about the perturbations in the airflow introduced by the presence of the device are collected, compared and analyzed. Taking advantage of the previous results, this leads to optimize the shape of device itself to have increased performance while introduce as less perturbations as possible. This step was already foreseen at the beginning because of the arbitrary choices taken in drawing the first device model, which had a very simple and intuitive design.

4.7.1   Flow analysis

For simplicity, in this section only the flow variables (in particular the velocity field and the streamlines) of the case B will be analyzed, because of its analogy with the case A: any conclusion that will follow will be applied to both cases.

Looking at the Figure 53, in which the velocity field and the streamlines crossing the filtering media are reported, several critical situations to work on are detected and highlighted (zone 1 to 5 in the figure).

- Zone 1: as already showed in the Figure 45 and Figure 46, just before the device inlet there is a zone of low velocity in which the flow detachment starts (point a). This is due to the presence of the filtering media that, because of its permeability feature, slows the air down creating this high-pressure zone at its inlet;

- Zone 2: the closed loops suggest the presence of a zone of high vorticity and very low velocity (almost zero) from where the air is neither entering nor exiting. This effect reduces the net air flow rate entering the capturing media, limiting so its efficiency and increases the drag force. Moreover, in this way after a working period, the filtering media will present non homogeneity due to a non uniform exposure to the pollutant: the upper part will tend to saturate faster;

- Zone 3: the arbitrary choice of the dimension and position of the outlet hole of the device generates a non optimal flow of the air outside. There is a zone with great velocity gradient with an acceleration (at the outlet hole) with a consequent deceleration (straight out of the device). The previously treated air is undesirably sent upward to the outside with a large y-component of velocity being so almost perpendicular to the device orientation;

- Zone 4: the separation of the streamlines in this zone sensibly affects the performance of the car: a portion of the processed air goes in opposite direction of the car motion;

- Zone 5: the wake past the device is almost inevitable and it starts at the beginning of the upper-frontal part of the device where the detachment of the flow occurs (point b).
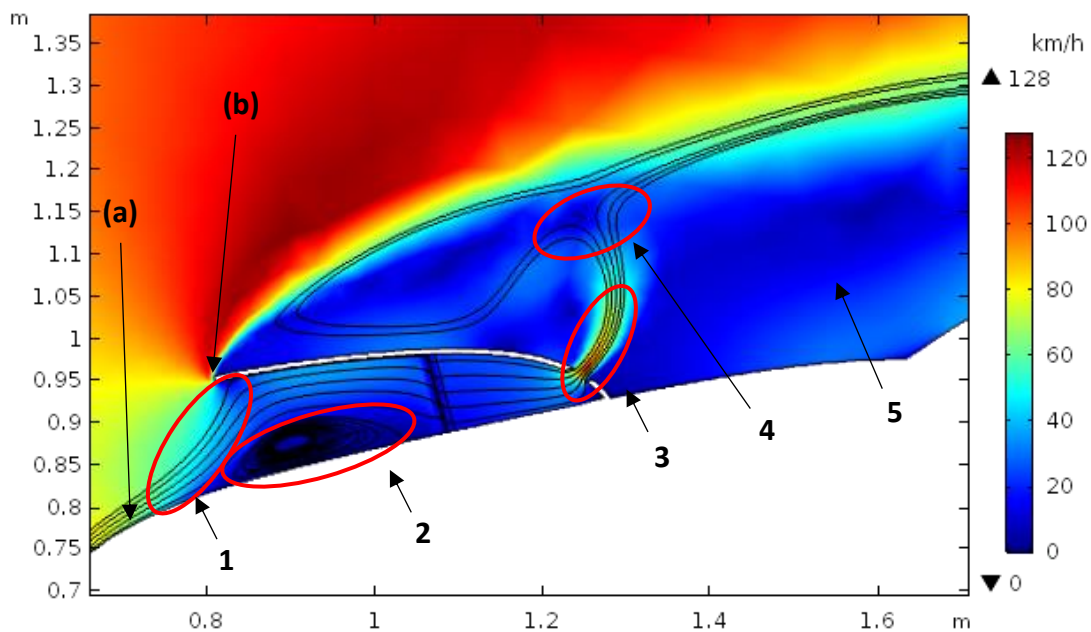
Figure 53 Local velocity magnitude field for Case B at car speed at car speed of 80 km/h

Davide Carlucci

4.7.2 Shape optimization (case C)

Detected the points of weakness of the first device design, corrective actions are done to try minimizing their negative effect and enhance the main indicators. At each problem presented before a remedial solution is proposed. Usually a solution for a problem affects indirectly, either positively or negatively, also the other parameters thus, only the overall result will be shown even if each modification is addressed mainly at one single problem.
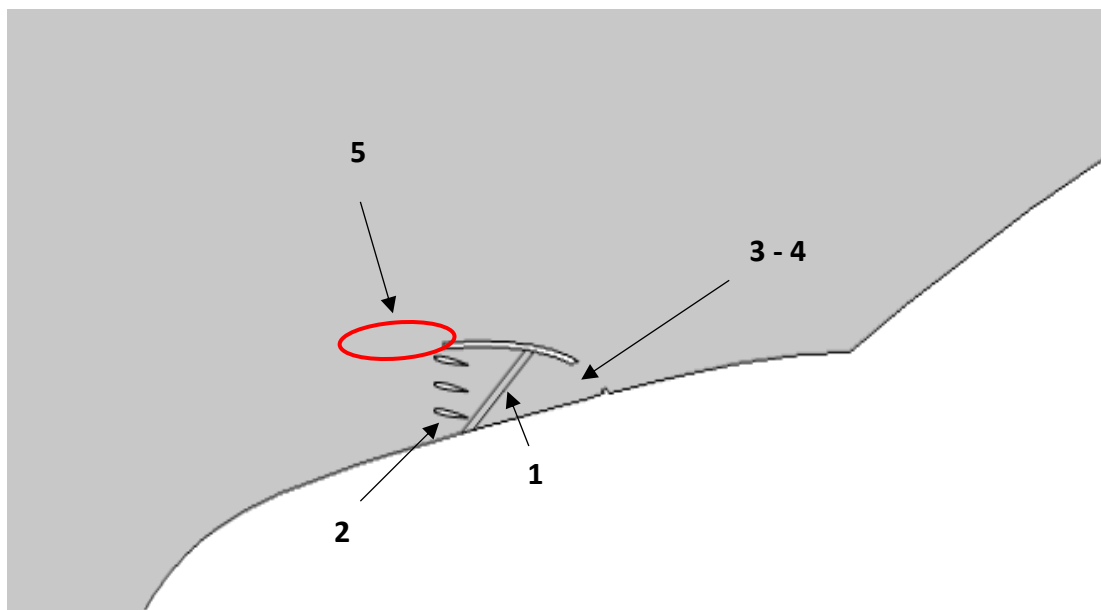
Figure 54 Device shape after optimization (Case C)

The adjustments brought are shown in the Figure 54.

These modifications are listed and their benefits are explained and plotted (Figure 55) as follows:

- Modification 1: the filtering media is tilted clockwise with an angle of 60°. By sloping it, the upper part faces the incoming flow later than how it did in the former design, delaying the detachment of the flow on the car silhouette;
- Modification 2: some thin airfoil-shaped deflectors are placed at the device inlet. The air is deflected downward eliminating so the prior high vorticity zone and

Davide Carlucci

letting the entire area of the filtering media to work by avoiding the air to accumulate only on the upper part;

- Modification 3-4: the outlet hole is now situated more down and it is bigger than before. The outflowing air is now not reflowing back at its exit and it goes also less upward than before, joining smoothly the high velocity zone;

- Modification 5: the length of the upper part of the device is sensibly reduced and with it also the wake dimension decreases enhancing the aerodynamic penetration of the system.
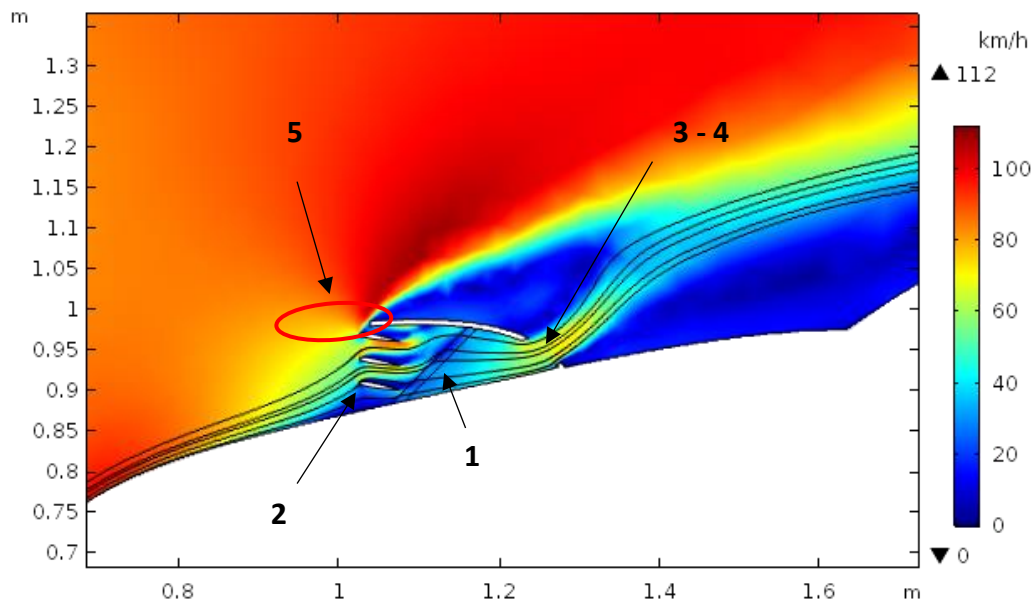
Figure 55 Local velocity magnitude field for Case C at car speed at car speed of 80 km/h

The main indicators, after the above-mentioned modifications, are calculated.

Table 6 Main indicators for the Case C (optimized hood mounting position)

Case C

C_d	0.369
A	1.344 m
C_dA	0.496 m
Δp	77.3 Pa
$\dot{V}$	1708.8 m²/h

It can be seen how the drag coefficient, as well as the drag area, is reduced (Table 6). The flow rate shows a big increment of around six times compared to the case B, which represented already a good result. As drawback the pressure drop decreases, if compared to the case B, but its value is still higher than the one in some sub-cases of the roof mounting position.

Davide Carlucci

5   CHAPTER 6: 3D SIMULATIONS

The previous 2D simulations have lead to the determination of the best device position on the car, as well as some suggestions on how to optimize the device shape itself. Starting from the obtained results, fewer different 3D simulations can be performed, with consequent time save. In all the simulations the car speed is 80 km/h, for the above-mentioned criteria. The extensive quantities are no longer divided by length units becoming so:

- Frontal area (A)[m^2]
- Drag area (C$_d$ A) [m^2]
- Air flow rate ($\dot{V}$)[m^3/h]

5.1   Reference case: 3D simulation

The first step, while proceeding towards the 3D study, consists in simulating the car alone, as already done with the 2D simulations. The aim is the same as before: to create the reference case for the following simulations.

5.1.1   Car 3D CAD creation

The 3D CAD model used for the following simulations has been created from the extrusion of the silhouettes of the three orthogonal views of the car.
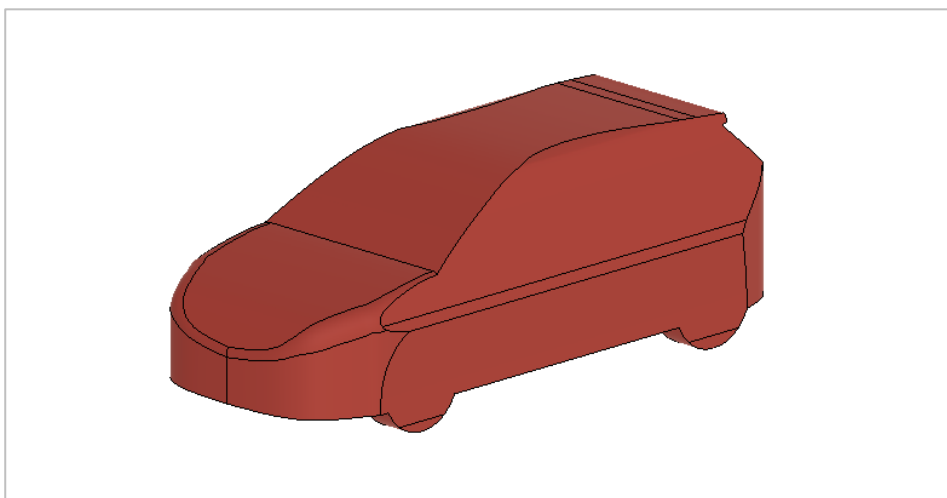
Figure 56 Simplified 3D car CAD

Davide Carlucci

In this way the model does not have all the details that an especially drawn CAD could have, and moreover, it is shaped as a single solid object (Figure 56). The rearview mirrors are removed, to avoid unnecessary complications, and the wheels are fixed to the car body and their rotation is neglected.

5.1.2 Simulation setup

The physics used are the same of the ones showed in the 2D simulations, as well as the rules for creating the computational domain. In addition, it is common practice to consider only half of the domain after having divided it in two identical halves along the longitudinal vertical plan. This is done because of the symmetry, both physical and geometrical, of the problem that lets the computation to be lighter and faster.
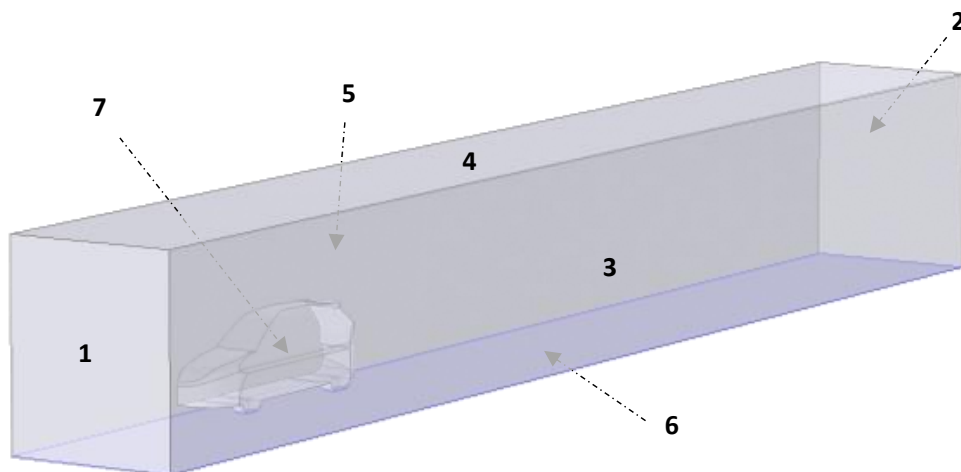
Figure 57 Domain dimensions for the 3D simulations

Regarding the boundary conditions, all the previous constraints are similarly applied to the COMSOL model, exception made for the ground, which is considered as a wall with relative movement, and the new generated longitudinal surface which needs a symmetry constraint (Figure 57).

Davide Carlucci

The following constraints are so applied for Turbulent Flow physics (spf):

- Boundary 1: Inlet - Normal inflow velocity (80 [km/h])
- Boundary 2: Outlet – Pressure (0 [Pa])
- Boundaries 3-4: Open Boundary – Normal stress (0 [N/m^2])
- Boundary 5: Wall – Symmetry
- Boundary 6: Wall – Wall condition – Sliding wall (80 [km/h])
- Boundary 7: Wall – Wall condition (no slip)

5.1.3   3D reference case results

A *Coarse* physics-controlled mesh is applied and the simulation converges after *6h 41m 53s*.

The main indicators are shown in the Table 7:

Table 7 Main indicators for the 3D reference case (only car)

3D Reference case

C_d	0.357
A	2.144 m^2
C_dA	0.765 m^2

The Drag coefficient value is in the range of the real one (0.357 computed vs. 0.35-0.36 real) while the Frontal Area issues a little overestimation (2.144 m^2 computed vs. 1.91 m^2 real) mainly due to the simplifications of the CAD model.

5.2   Device redesign

The 2D design of the device was mainly focused on its longitudinal shape, because of the nature of the simulation itself. While moving towards the 3D simulation, the flow phenomena around the device sides start to be relevant to be studied and optimized: a slightly different device has to be drawn to accomplish this purpose. The device has been

already optimized in the case C, though in a simple way, according to what emerged from the flow analysis performed on the case B, but a further reshape is done.
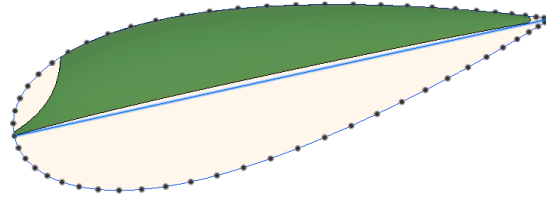
Figure 58 NACA 4412 airfoil (dotted blue line) circumscribed in the device lateral view

To redesign in a more efficient way the device, inspiration is taken from the NACA airfoils, widely used in the aeronautic field for aircraft wings and aerodynamic appendices. NACA (National Advisory Committee for Aeronautics) created various standard equations that need few parameters to generate the airfoil shape. The 4-digits series, in particular the 4412 one, is the one chosen as starting point for the drawing Figure 58. The choice is justified by the fact that this airfoil is symmetrical and has good proportion between height and length.
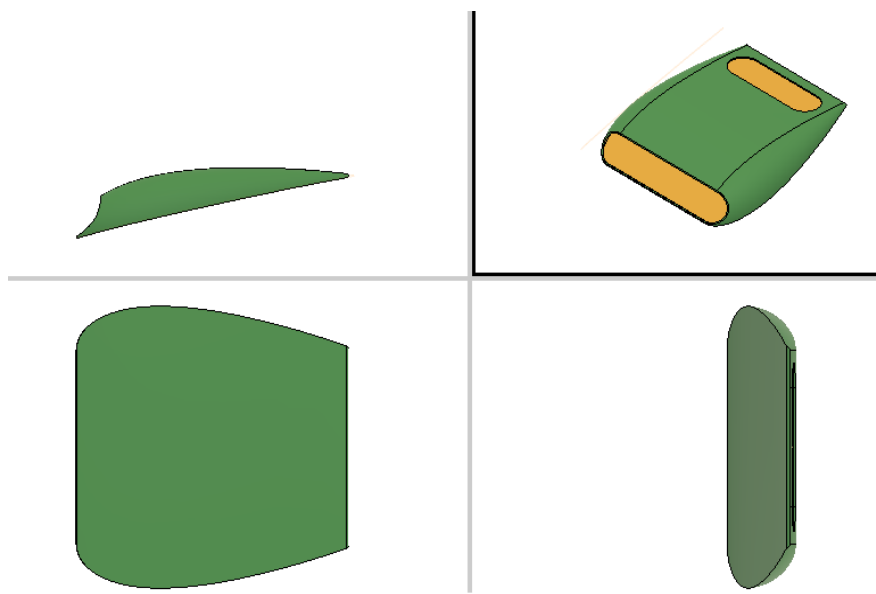
Figure 59 Device CAD (version 2) with different views

Davide Carlucci

The 4412 airfoil is used also to shape the lateral part of the device. After the complete modelling, the device appears as in Figure 59. The device size is arbitrary but it has been designed taking into account the ease of handling and mounting by a single person. The filtering media is then drawn in COMSOL, identically as done in the case C.

5.3 System 3D simulations

Two different versions of the same device will be simulated: the simple one (case D) and one with the internal deflectors (case E).
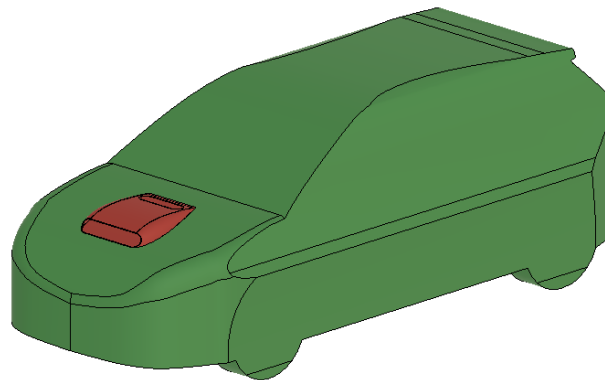
Figure 60 System 3D CAD (car + device)

In both cases the device is placed on the car hood, in a central position, to be simulated (Figure 60). For the *Free Flow in Porous Media* (fp) the same boundary conditions, as in the previous 2D cases, are applied.

5.3.1 Device case D: simple 3D

In this case the device lacks of the internal deflectors, used in the case C. This case is needed as a base case to understand the performance enhancement brought by the deflectors in the 3D simulations.

An *Extremely Coarse* physics-controlled mesh is used and the simulation converges in 2*h 3min 40s*.

Davide Carlucci

The main indicators are shown in the Table 8:

Table 8 Main indicators for the case D (3D simple)

Case D

C_d	0.404
A	2.144 m^2
C_dA	0. 866 m^2
Δp	40.8 Pa
$\dot{V}$	83.1 m^3/h

The Drag Coefficient, as well as the Drag Area, is now +13% higher than the reference case. The pressure drop is lower than the 2D case, because of the more extreme device shape.
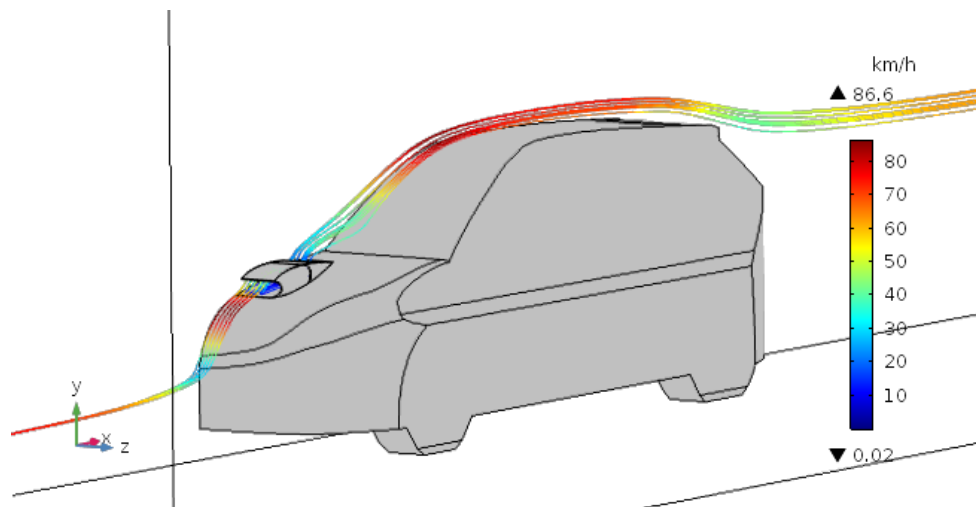
Figure 61 Streamlines crossing the device with correspondent velocity magnitude

In the Figure 61 it is shown as the streamlines crossing the device start at relatively low height, being so able to better capture the direct emissions from preceding vehicles. From the colour pattern is visible how the air slows down while entering the device, for later accelerate at its exit.

Davide Carlucci

5.3.2 Device case E: optimized 3D with deflectors

The only difference between the case D and the case E consists in the presence of internal deflectors to reduce the drag force, as done in the case C.
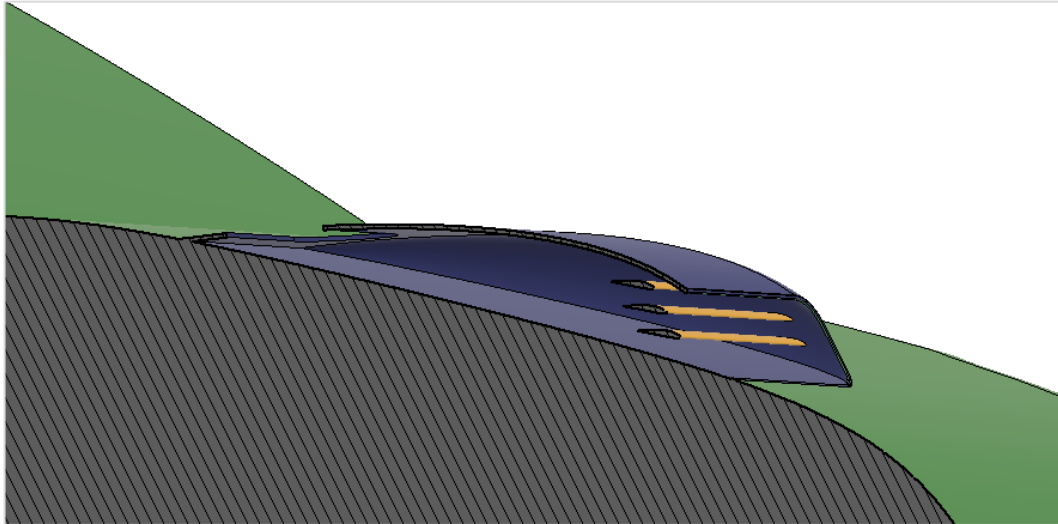
Figure 62 Device cross section showing the three deflectors (yellow)

The purpose of the deflectors is to force more air to enter into the device (Figure 62), increasing air the flow rate and so the pollutants captured. Because of the thin dimension of the deflectors, a *Coarse* physics-controlled mesh is used and the simulation converges in 59*h 28min 5s*.

The main indicators are reported in Table 9.

Table 9 Main indicators for the case E (3D optimized)

Case E	
C_d	0.366
A	2.144 m^2
C_dA	0. 784 m^2
Δp	40.0 Pa
$\dot{V}$	112.3 m^3/h

Davide Carlucci

The Drag Area is +2% higher than the reference case. The pressure drop is almost the same as in the case D while the air flow rate is slightly higher (+35%) compared to the case without deflectors.

Davide Carlucci

6 CHAPTER 6: FUEL ECONOMY AND FEASIBILITY

After performing several simulations on the device behavior, the feasibility of the device has to be investigated. The calculated parameters, especially the Drag Area and the Flow Rate, will be used to estimate the losses introduced by the devices and the pollutant capturing rate: the aerodynamic losses will affect the fuel economy of the vehicles while the capturing rate will justify or not the utility of the device. The aim is, in fact, for the device to collect a bigger amount of pollutants than the one that its presence generates by introduction of aerodynamic losses. For this purpose the average fuel economy and emissions estimation, together with an analysis on the car fleet composition, have to be done.

6.1 Vehicles emission European regulations

The real average cars emission is a difficult parameter to estimate, being each car exposed to different duty loads and maintenance. Several European Union directives for passenger car emission limits have been enacted in the past years. All the vehicles sold in EU shall respect the existing regulation at the moment during which the car is launched into the market. The guideline follows a progressive numeration being Euro 1 the oldest and Euro 6 the latest.

Table 10 European emissions regulation classes (in g/km, exception made for PN in number/km) [29]

Tier	Date (1st reg.)	CO	THC	NMHC	NOx	HC+NOx	PM	PN*
DIESEL								
Euro 1	01/1993	2.72	-	-	-	0.97	0.14	-
Euro 2	01/1997	1.0	-	-	-	0.7	0.08	-
Euro 3	01/2001	0.66	-	-	0.50	0.56	0.05	-
Euro 4	01/2006	0.50	-	-	0.25	0.30	0.025	-
Euro 5a	01/2011	0.50	-	-	0.180	0.230	0.005	-
Euro 5b	01/2013	0.50	-	-	0.180	0.230	0.0045	6×10^{11}
Euro 6	09/2015	0.50	-	-	0.080	0.170	0.0045	6×10^{11}
PETROL								
Euro 1	01/1993	2.72	-	-	-	0.97	-	-
Euro 2	01/1997	2.2	-	-	-	0.5	-	-
Euro 3	01/2001	2.3	0.20	-	0.15	-	-	-
Euro 4	01/2006	1.0	0.10	-	0.08	-	-	-
Euro 5a	01/2011	1.0	0.10	0.068	0.060	-	0.005	-
Euro 5b	01/2013	1.0	0.10	0.068	0.060	-	0.0045	-
Euro 6	09/2015	1.0	0.10	0.068	0.060	-	0.0045	6×10^{11}

Davide Carlucci

(CO=Carbon Oxide, THC=Total Hydrocarbons, NMHC=Non-Methane Hydrocarbons, NO$_x$=Nitrogen Oxides, PM=Particulate Matter, PN=Particles Number)

The Table 10 [29] shows the limits issued for each category, expressed in g/km (*exception made for Particles Number, PN, that is measured in "number/km"):

6.2   Passenger cars identification in Spain by emission

A Spanish identification system, to differentiate the road vehicles based on their emission levels, has been created by *Dirección General de Tráfico* (DGT), the government department responsible for the Spanish road transport network. Even if their application in the cars is still not strictly compulsory and ruled, their use is highly recommended in metropolitan areas as well as in Barcelona to avoid fines during traffic circulation restriction resulting from high concentration of pollutants.

Figure 63 Spanish Eco-labels for vehicles emission identification

There are four different labels (Figure 63) that incorporate the following vehicles [30]:

- **Zero**: battery electric vehicles (BEV), plug-in hybrid electric vehicles (PHEV), range-extended electric vehicles (REEV) and fuel cell electric vehicles (FCEV) with an autonomy larger than 40 km;
- **Eco**: PHEV with an autonomy smaller than 40 km, hybrid electric vehicles (HEV), compressed natural gas vehicles (CNG), liquefied petroleum gas vehicles (LPG) that have to respect anyway the standard of C-labeled vehicles;

- **C**: diesel vehicles Euro 6 and petrol vehicles Euro 4, 5 and 6;
- **B**: diesel vehicles Euro 4 and 5 and petrol vehicles Euro 3;
- All the diesel-powered vehicles registered before 2006 and the petrol ones before 2000 do not have the right to get a label, due to their high emission levels

6.3 Car fleet in Barcelona province and Barcelona city

A bibliographic investigation on passenger car fleet in Barcelona is carried and the data from different sources are compared. When there is no direct data from Barcelona municipality itself the data are then extracted at provincial level.
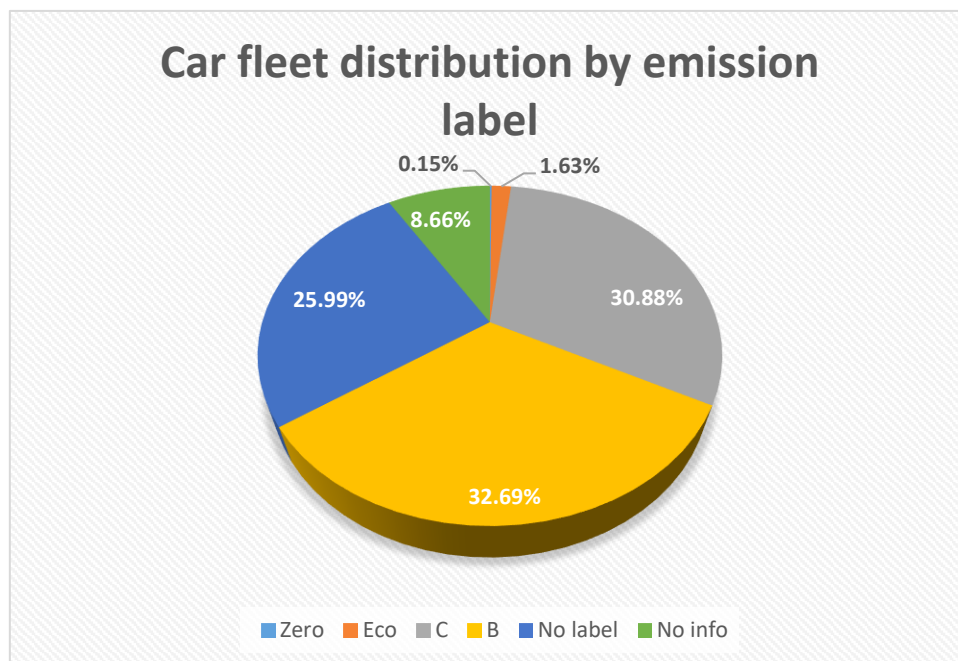

Figure 64 Car fleet distribution by emission label in Barcelona province

Table 11 Car fleet distribution by emission label in Barcelona province

	Zero	Eco	C	B	No label	No info	*TOTAL*
No. cars	3693	40355	764900	809784	643650	214428	*2476810*
Percentage	0,15%	1,63%	30,88%	32,69%	25,99%	8,66%	*100.00%*

Provincial statistics are obtained by DGT through its website: the car distributions by emission label and fuel type in Barcelona province are reported in Figure 64, according

Davide Carlucci

to the 2018 annual report (Table 11) [31]. Around 2.5 millions cars are registered in the province.
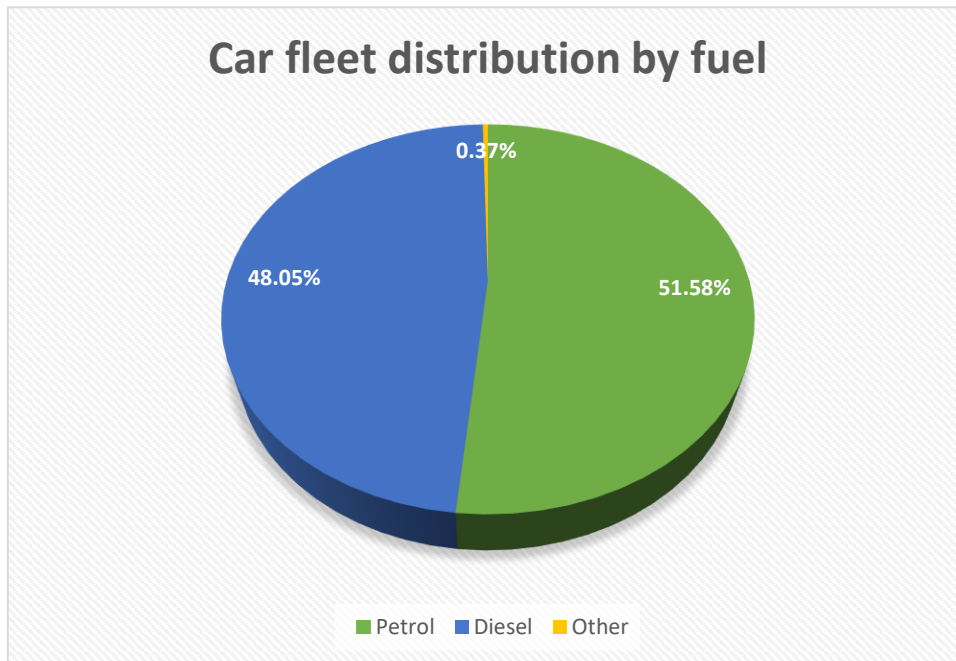

Figure 65 Car fleet distribution by fuel in Barcelona province

Table 12 Car distribution by fuel in Barcelona province

	Petrol	Diesel	Other	*TOTAL*
Percentage	51.58%	48.05%	0.37%	*100.00%*
No. cars	1277560	1189993	9257	*2476810*

Since in each label category, different kinds of propulsion can be found, also characterization by propulsion is done; being also dissimilar the regulations for each type of fuel within the same label. Petrol powered cars appeared to be slightly more (+3.5%) than the diesel ones, while the alternative fuels reach less than ten thousands vehicles (Figure 65 and Table 12).

Solely in Barcelona city there are 560791 passenger cars registered accounting so for 22.64% of the passenger cars of the entire province, according to same data.

Davide Carlucci

6.4 Average pollutants emissions estimation

An estimation of the average pollutants emission per car per kilometer is made, starting from the previously Eco-labelling data. In order to mitigate the errors, attributable to vague assumptions and lack of precise data, all the values given in a range are, at this stage, considered toward both an overestimation and underestimation of the emissions. It is therefore assumed that:

- The data taken at provincial level are mirrored to the ones at city level;
- The vehicles belonging to the labels Zero and Eco, being only 1.78% of the share, will be neglected in the calculation, given also their low emission level;
- The vehicles powered by alternative fuels (others than petrol or diesel), being only 0.37% of the share, will be neglected in the calculation, given also their low emission level;
- The resulting new distribution of fuel is 51.76% diesel and 48.24% petrol;
- The vehicle propulsion distribution is uniform in each label of emission (51.76% diesel-48.24% petrol);
- In a label identification, if more than one Euro category is considered, the stricter category is considered in the underestimated emissions (e.g. in label C, the petrol cars are all considered Euro 6) and contrariwise for the overestimated ones;
- The vehicles with no label and the ones with no info are considered petrol Euro 2 or diesel Euro 3 for the underestimated emissions or both Euro 1 for the overestimated ones;
- The THC and NMHC are considered together into the category o HC.

Table 13 Emissions estimation for Barcelona car fleet

EMISSIONS (g/km)	CO	NO$_x$	PM	HC
Underestimated	1.1833	0.1940	0.0130	0.1514
Overestimated	**1.6479**	**0.2091**	**0.0330**	**0.2959**

After all these considerations the car fleet emissions (in g/km) are calculated as in Table 13. Regarding the NO$_x$, there are no major differences between the two obtained values, meaning that the regulations were consistent along the years, unlike the other pollutants. Anyway, for the feasibility study, the overestimated values will be considered

Davide Carlucci

from now on. Moreover, since from the air quality data analyzed before there are no info about Carbon monoxide and Hydrocarbons concentration, the further discussion will consider Nitrogen oxides and Particulate matter only.

6.5 Aerodynamic influence on pollutants emissions

The losses introduce by the presence of the device are merely aerodynamics. It is important so to know how these losses affect the overall car fuel consumption and emissions.

According to an US Department of Energy study [32], around 5% of the fuel energy is dissipated due to aerodynamics friction in the urban cycle.

Being the aerodynamics power losses defined as:

$$P_{L,aero} = F_D \cdot v = \frac{1}{2}\rho C_D A v^3$$

it can be seen how the losses are linearly proportional to the Drag Area (C_d*A). An increase in the Drag Area of +13%, like in the case D, or of +2%, case E, will increase so the aerodynamic losses respectively of these amounts.

The emissions introduced are calculated as:

$$Emissions_{introduced} = Emissions_{TOT} \cdot \frac{P_{L,aero}}{P_{TOT}} \cdot \frac{C_D A}{C_{D,ref} A}$$

Where the terms in the equation are defined as:

- $Emissions_{introduced}$: emissions increase due to device presence (Table 14);
- $Emissions_{TOT}$: car overall average emissions without device (Table 13);
- $\frac{P_{L,aero}}{P_{TOT}}$: ratio between the aerodynamic power losses and the total fuel power (assumed as 5%) ;
- $\frac{C_D A}{C_{D,ref} A}$: increase in Drag Area due to the device presence.

Table 14 Emissions introduced by the presence of the device

EMISSIONS$_{introduced}$ (mg/km)	NO$_x$	PM
Case D	1.36	0.21
Case E	0.21	0.03

The emissions showed in Table 14 are the emissions introduced by the effect of the device. These values represents so the minimum amount of pollutants which have to be captured to make the device feasible.

The other assumptions made to evaluate the feasibility of the device are:

- The 3D simulations have been performed at a car speed of 80 km/h, so all the further consideration will take into account this factor. It is well known that the aerodynamics losses have a bigger weight on the overall losses at increasing car speed.
- The capturing efficiency is of 100%, meaning that all the pollutants entering the device are captured.
- The flow rates of air treated are the ones calculated in the case D and E.
- The pollutants concentration in air is assumed equal to the limit one (90 µg/m^3 for NO$_x$ and 35 µg/m^3 for PM). Even if the limits are sometimes exceeded, the days in which the limits are not exceeded are still more, so an averaged level would underestimate the actual level of pollution at ground level due to actual car flue gases streams.

The pollutants captured per kilometer [mg/km] can be calculated as follows:

$$Pollutants_{captured} = \frac{\dot{V} \cdot x_P}{1000 \cdot v}$$

Where:

- $\dot{V}$ is the air flow rate entering the device [m^3/h];
- x_P is the pollutants concentration [µg/m^3];
- v is the car speed [km/h].

The calculated theoretical amount of pollutants captured can be estimated.

Davide Carlucci

Table 15 Particles capture in case D and E (underlined the acceptable values)

PARTICLES$_{captured}$ (mg/km)	NO$_x$		PM	
Case D	0.09 (-93%)	✗	0.04 (-81%)	✗
Case E	0.13 (-38%)	✗	0.05 (+67%)	✓

The values obtained (

Table 15) are compared to the emissions increase shown in the Table 14. For the case D the amount of pollutants captured, both NOx (-94%) and PM (-81%), is never enough to justify the use of the device whereas for the case E, only the value of particulate matter trapped is more than the introduced one (+67%). This mean that, with the actual configuration, the given assumptions and simulations results, the device does not collect enough pollutants to justify its employment.

Davide Carlucci

7 CONCLUSIONS

A device for passive air cleaning from pollutants, using the impregnated activated carbon technology, has been designed and simulated through a CFD model, both in 2D and 3D, to evaluate its feasibility in terms of pollutants captured-emitted balance. The 2D simulations results defined the hood mounting position as the one with highest efficacy compared to the roof mounting position, because of its increased air flow rate and reduced drag coefficient. An optimized version of the device (airfoil shape, presence of deflectors, tilted filtering media) has been simulated in the 3D model with the aim of evaluating the air flow of air treated and the aerodynamic losses introduced while installed on the hood of a common car. After estimating the emissions caused by the presence of the device, the maximum amount of pollutants captured has been calculated and the two values have been compared. The results showed that, at this stage of development, the system is not able to capture a sufficient amount of pollutants to legitimize its use.

This Thesis has to be intended has a preliminary theoretical work, whose main purpose is to lay the foundations for a further, an more detailed, investigation. The path towards a final assessment on the real feasibility of the product has to pass through experimental analysis on the filtering media, for the determination of its main parameters (permeability and porosity) and its capturing performance with different pollutants. A further optimization of the shape of the apparatus, as well as an increased area of the filtering media, could also lead to better results.

Davide Carlucci

Davide Carlucci

BIBLIOGRAPHY

[1] C. Blanchar, "El País - Barcelona pierde la batalla contra la contaminación," 2 March 2019. [Online]. Available: https://elpais.com/ccaa/2019/03/02/catalunya/1551550337_084747.html. [Accessed July 2019].

[2] "World Health Organization," 2 May 2018. [Online]. Available: https://www.who.int/news-room/fact-sheets/detail/ambient-(outdoor)-air-quality-and-health. [Accessed July 2019].

[3] "Wikipedia," 24 June 2019. [Online]. Available: https://en.wikipedia.org/wiki/Nitrogen_oxide#Atmospheric_sciences. [Accessed July 2019].

[4] Jordan Hanania, Kailyn Stenhouse, Jasdeep Toor, Jason Donev, "Energy Education - Nitrogen oxide," 18 September 2015. [Online]. Available: https://energyeducation.ca/encyclopedia/Nitrogen_oxide. [Accessed July 2019].

[5] Jordan Hanania, Ellen Lloyd, Kailyn Stenhouse, Jasdeep Toor, Jason Donev, "Energy Education - Sulfur oxides," 28 September 2017. [Online]. Available: https://energyeducation.ca/encyclopedia/Sulfur_oxides. [Accessed July 2019].

[6] World Health Organization, WHO Air quality guidelines for particulate matter, ozone, nitrogen dioxide and sulfur dioxide, 2005.

[7] Generalitat de Catalunya, "Què és l'Índex Català de Qualitat de l'Aire?," 29 July 2015. [Online]. Available: http://mediambient.gencat.cat/ca/05_ambits_dactuacio/atmosfera/qualitat_de_laire/avaluacio/icqa/que_es_lindex_catala_de_qualitat_de_laire/index.html. [Accessed July 2019].

[8] "Open Data BCN," [Online]. Available: https://opendata-ajuntament.barcelona.cat/data/en/organization/medi-ambient?q=air&sort=fecha_publicacion+desc. [Accessed July 2019].

[9] "AFPRO® Filters - The principles of air filtration," [Online]. Available: https://www.afprofilters.com/the-principles-of-air-filtration/. [Accessed July 2019].

[10] "Donaldson Filtration Solutions - FAQs," [Online]. Available: https://www3.donaldson.com/en/gasturbine/support/faq.html. [Accessed July 2019].

[11] Allison Bailes, "Energy Vanguard," 24 October 2018. [Online]. Available: https://www.energyvanguard.com/blog/7-reasons-your-filter-isnt-improving-your-indoor-air-quality. [Accessed July 2019].

[12] Wladyslaw J. Kowalski, William Parry Bahnfleth, "MERV Filter Models for Aerobiological Applications," January 2002. [Online]. Available: https://www.researchgate.net/figure/Composite-of-all-MERV-filter-models-based-on-initial-conditions_fig3_237558312. [Accessed July 2019].

[13] "Oxbow - Understanding the difference between different types of activated carbon," [Online]. Available: http://www.oxbowactivatedcarbon.com/knowledgecenter/38. [Accessed July 2019].

[14] Henry Nowicki, George Nowicki, "Water Technology - The basics of activated carbon," 1 February 2016. [Online]. Available: https://www.watertechonline.com/the-basics-of-activated-carbon-adsorption/. [Accessed July 2019].

[15] "General Carbon Corporation - FAQs," [Online]. Available: http://generalcarbon.com/facts-about-activated-carbon/activated-carbon-faq/. [Accessed July 2019].

[16] "Thomas - Producing activated carbon," [Online]. Available: https://www.thomasnet.com/articles/chemicals/producing-activated-carbon. [Accessed July 2019].

[17] "Cameron Carbon Incorporated - Mesh chart size," [Online]. Available: http://www.uaecement.com/res/pdf/mesh-sizes.pdf. [Accessed July 2019].

[18] "HAYCARB - Activated Carbons Basics," [Online]. Available: https://www.haycarb.com/activated-carbon. [Accessed July 2019].

[19] "Chemviron - Activated Carbon," [Online]. Available: https://www.chemviron.eu/products/activated-carbon/. [Accessed July 2019].

[20] "Emis - Activated carbon adsorption," [Online]. Available: https://emis.vito.be/en/techniekfiche/activated-carbon-adsorption. [Accessed July 2019].

[21] "Magnaflux - Product Data Sheet," [Online]. Available: https://eu.magnaflux.com/product-solutions/liquid-penetrant-inspection/cleaners/lpi-chemicals-activated-carbon/product-data-sheet/. [Accessed July 2019].

[22] Jin Zhequan, Tian Bo, Wang Liwei, Wang Ruzhu , "Comparison on Thermal Conductivity and Permeability of Granular and Consolidated Activated Carbon for Refrigeration," *Chines Journal of Chemical Engineering,* vol. 21, pp. 676-682, 2013.

[23] L. Spurzem, "Wikimedia Commons - VW Golf V," 16 November 2006. [Online]. Available: https://commons.wikimedia.org/wiki/File:VW_Golf_V_-_2006-11-18_ret.jpg. [Accessed July 2019].

Davide Carlucci

[24] F. Gemelli, "Motor1 - TOP 20, le auto più vendute d'Europa nel 2018," 21 February 2019. [Online]. Available: https://it.motor1.com/news/306131/auto-piu-vendute-meno-vendute-europa-2018/. [Accessed July 2019].

[25] S. Amadoz, "El motor - Las estadísticas más inesperadas sobre los coches españoles," 21 December 2018. [Online]. Available: https://motor.elpais.com/actualidad/estadisticas-curiosas-coches-en-espana/. [Accessed July 2019].

[26] "L.E. Mayfield," [Online]. Available: http://www.mayfco.com/dragcd~1.htm. [Accessed July July].

[27] S. Dobie, "Topgear - Volkswagen quits World Rally Championship," 2 November 2016. [Online]. Available: https://www.topgear.com/car-news/motorsport/volkswagen-quits-world-rally-championship. [Accessed July 2019].

[28] "HDfondos," [Online]. Available: http://www.hdfondos.eu/preview/453397/3750/3000. [Accessed July 2019].

[29] "Wikipedia - European emission standards," 26 June 2019. [Online]. Available: https://en.wikipedia.org/wiki/European_emission_standards#Emission_standards_for_passenger_cars. [Accessed July 2019].

[30] "BOLETÍN OFICIAL DEL ESTADO n.96 - 3828," 21 April 2016. [Online]. Available: http://www.dgt.es/Galerias/seguridad-vial/distintivo-ambiental/BOE-A-2016-3828.pdf. [Accessed July 2019].

[31] "DGT - Tablas estadísticas 2018," [Online]. Available: http://www.dgt.es/es/seguridad-vial/estadisticas-e-indicadores/parque-vehiculos/tablas-estadisticas/2018/. [Accessed July 2019].

[32] "Fuel economy - Where the Energy goes: Gasoline vehicles," [Online]. Available: https://www.fueleconomy.gov/feg/atv.shtml. [Accessed July 2019].

LIST OF FIGURES

LIST OF TABLES

APPENDIX A – MATLAB script

Contents

Initialization

```matlab
clearvars        % Clearing all the variables
close all        % Closing all the figures
clc              % Clearing the COMMAND WINDOW
tic              % Initialising the timer
```

Parameters

```matlab
o3_l=110;    %µg/m³ (Ozone limit level)
no2_l=90;    %µg/m³ (Nitrogen dioxide limit level)
pm10_l=35;   %µg/m³ (PM10 limit level)
```

Weather data

```matlab
prec1=xlsread("weather_bcn1.xlsx",'A:A');
day1=datetime(xlsread("weather_bcn1.xlsx",'B:B'),'ConvertFrom',"excel","Format","dd-MMM-uuuu");

prec2=xlsread("dcarlucci.01.xlsx",'G:G');
day2=datetime(xlsread("dcarlucci.01.xlsx",'B:B'),'ConvertFrom',"excel","Format","dd-MMM-uuuu HH:mm:ss");
```

Main script

```matlab
[file,path]=uigetfile('*.csv','Select the file to analyse');       % Choose the file to analyse
filename=sprintf('%s%s',path,file);                                % Getting the file to analyse

data1= table2struct(readtable(filename,'FileEncoding','UTF-8','TreatAsEmpty',{'"--
"','"NA"','Na','NA','N/A'},'DatetimeType','text'));
opt_data1=detectImportOptions(filename);                           % Saving the Import Options of the file .csv

cabin=strings(length(data1),1);
qualitat_aire=strings(length(data1),1);
codi_dtes=strings(length(data1),1);
zqa=strings(length(data1),1);
codi_eoi=strings(length(data1),1);
qualitat_o3=strings(length(data1),1);
hora_o3=zeros(length(data1),1);
```

```matlab
valor_o3=zeros(length(data1),1);
o3_index=0;
qualitat_no2=strings(length(data1),1);
hora_no2=zeros(length(data1),1);
valor_no2=zeros(length(data1),1);
no2_index=0;
qualitat_pm10=strings(length(data1),1);
hora_pm10=zeros(length(data1),1);
valor_pm10=zeros(length(data1),1);
pm10_index=0;
generat=strings(length(data1),1);
% generat=datetime(strings(length(data1),1),'Format','dd/MM/yyyy H:mm');

station(9,:)=struct('qualitat_aire',[],'codi_dtes',[],'zqa',[],'codi_eoi',[],'qualitat_o3',[],'hora_o3',[],'valor_o3',[],'limit_o3',[],'qualitat_no2',[],'hora_no2',[],'valor_no2',[],'limit_no2',[],'qualitat_pm10',[],'hora_pm10',[],'valor_pm10',[],'limit_pm10',[],'generat',[]);

for ii=1:length(data1)  % Extraction and correction of the data

    %O3-----------------------------------------------------------%
    if(data1(ii).hora_o3(end)=='h')                    % Eliminating the 'h' from the 'hora'
        data1(ii).hora_o3(end)='';
    elseif(data1(ii).hora_o3(end)=='A'||'-')           % Eliminating the 'NA' and '--' from the 'hora'
        data1(ii).hora_o3(:)='';
    end

    hora_o3(ii)=str2double(convertCharsToStrings(data1(ii).hora_o3())); % Converting the hour from string to number

    if(((data1(ii).qualitat_o3(end)=='A')&&(data1(ii).qualitat_o3(1)=='N'))||(data1(ii).qualitat_o3(end)=='-')) %
Eliminating the 'NA' and '--' from the 'qualitat'
        data1(ii).qualitat_o3(:)='';
    end

    if(((data1(ii).valor_o3(end)=='A')&&(data1(ii).valor_o3(1)=='N'))||(data1(ii).valor_o3(end)=='-'))  % Eliminating the
'NA' and '--' from the 'valor'
        data1(ii).valor_o3(:)='';
    else
        data1(ii).valor_o3(end-4:end)='';   % Eliminating the 'µg/m³' from the 'valor'
        if(~isempty(data1(ii).valor_o3()))
            data1(ii).valor_o3(end)='';     % Eliminating the ' ' (space) from the 'valor'. There are some cells that have only
'µg/m³', that's why it was not possible to do this in the previous step
        end
    end

    valor_o3(ii)=str2double(convertCharsToStrings(data1(ii).valor_o3()));   % Converting the 'valor' from string to
number

    if(valor_o3(ii)>=o3_l)  % Checking if the limit is respected
        o3_index=o3_index+1;
    end

    %NO2-----------------------------------------------------------%
    if(data1(ii).hora_no2(end)=='h')          % Eliminating the 'h' from the 'hora
        data1(ii).hora_no2(end)='';
    elseif(data1(ii).hora_no2(end)=='A'||'-')  % Eliminating the 'NA' and '--' from the 'hora'
        data1(ii).hora_no2(:)='';
    end

    hora_no2(ii)=str2double(convertCharsToStrings(data1(ii).hora_no2()));   % Converting the hour from string to
number
```

```matlab
    if(((data1(ii).qualitat_no2(end)=='A')&&(data1(ii).qualitat_no2(1)=='N'))||(data1(ii).qualitat_no2(end)=='-')) % Eliminating the 'NA' and '--' from the 'qualitat'
        data1(ii).qualitat_no2(:)='';
    end

    if(((data1(ii).valor_no2(end)=='A')&&(data1(ii).valor_no2(1)=='N'))||(data1(ii).valor_no2(end)=='-')) % Eliminating the 'NA' and '--' from the 'valor'
        data1(ii).valor_no2(:)='';
    else
        data1(ii).valor_no2(end-4:end)=''; % Eliminating the 'µg/m³' from the 'valor'
        if(~isempty(data1(ii).valor_no2()))
            data1(ii).valor_no2(end)='';   % Eliminating the ' ' (space) from the 'valor'. There are some cells that have only 'µg/m³', that's why it was not possible to do this in the previous step
        end
    end

    valor_no2(ii)=str2double(convertCharsToStrings(data1(ii).valor_no2())); % Converting the 'valor' from string to number

    if(valor_no2(ii)>=no2_l)  % Checking if the limit is respected
        no2_index=no2_index+1;
    end

    %PM10------------------------------------------------------------%
    if(data1(ii).hora_pm10(end)=='h')          % Eliminating the 'h' from the 'hora
        data1(ii).hora_pm10(end)='';
    elseif(data1(ii).hora_pm10(end)=='A'||'-') % Eliminating the 'NA' and '--' from the 'hora'
        data1(ii).hora_pm10(:)='';
    end

    hora_pm10(ii)=str2double(convertCharsToStrings(data1(ii).hora_pm10())); % Converting the hour from string to number

    if(((data1(ii).qualitat_pm10(end)=='A')&&(data1(ii).qualitat_pm10(1)=='N'))||(data1(ii).qualitat_pm10(end)=='-')) % Eliminating the 'NA' and '--' from the 'qualitat'
        data1(ii).qualitat_pm10(:)='';
    end

    if(((data1(ii).valor_pm10(end)=='A')&&(data1(ii).valor_pm10(1)=='N'))||(data1(ii).valor_pm10(end)=='-')) % Eliminating the 'NA' and '--' from the 'valor'
        data1(ii).valor_pm10(:)='';
    else
        data1(ii).valor_pm10(end-4:end)=''; % Eliminating the 'µg/m³' from the 'valor'
        if(~isempty(data1(ii).valor_pm10()))
            data1(ii).valor_pm10(end)='';   % Eliminating the ' ' (space) from the 'valor'. There are some cells that have only 'µg/m³', that's why it was not possible to do this in the previous step
        end
    end

    valor_pm10(ii)=str2double(convertCharsToStrings(data1(ii).valor_pm10()));  % Converting the 'valor' from string to number

    if(valor_pm10(ii)>=pm10_l)  % Checking if the limit is respected
        pm10_index=pm10_index+1;
    end

    % Putting the data read from the CSV file to auxiliary arrays in the proper format
    cabin(ii)=convertCharsToStrings(data1(ii).nom_cabina());
    qualitat_aire(ii)=convertCharsToStrings(data1(ii).qualitat_aire());
    codi_dtes(ii)=convertCharsToStrings(data1(ii).codi_dtes());
    zqa(ii)=convertCharsToStrings(data1(ii).zqa());
```

```matlab
codi_eoi(ii)=convertCharsToStrings(data1(ii).codi_eoi());
qualitat_o3(ii)=convertCharsToStrings(data1(ii).qualitat_o3());
qualitat_no2(ii)=convertCharsToStrings(data1(ii).qualitat_no2());
qualitat_pm10(ii)=convertCharsToStrings(data1(ii).qualitat_pm10());
generat(ii)=(data1(ii).generat());

% Dividing data for each one of the eight "cabin" by putting the proper field of the 'station' struct
switch cabin(ii)
    case 'Barcelona - Sants'
        station(1).qualitat_aire(end+1)=qualitat_aire(ii);
        station(1).codi_dtes(end+1)=codi_dtes(ii);
        station(1).zqa(end+1)=zqa(ii);
        station(1).codi_eoi(end+1)=codi_eoi(ii);
        station(1).qualitat_o3(end+1)=qualitat_o3(ii);
        station(1).hora_o3(end+1)=hora_o3(ii);
        station(1).valor_o3(end+1)=valor_o3(ii);
        station(1).qualitat_no2(end+1)=qualitat_no2(ii);
        station(1).hora_no2(end+1)=hora_no2(ii);
        station(1).valor_no2(end+1)=valor_no2(ii);
        station(1).qualitat_pm10(end+1)=qualitat_pm10(ii);
        station(1).hora_pm10(end+1)=hora_pm10(ii);
        station(1).valor_pm10(end+1)=valor_pm10(ii);
        %        station(1).generat(end+1)=generat(ii);
        station(1).limit_o3(end+1)=o3_l;
        station(1).limit_no2(end+1)=no2_l;
        station(1).limit_pm10(end+1)=pm10_l;
        station(1).generat(end+1)=datetime(generat(ii),'Format','dd/MM/yyyy H:mm');
    case 'Barcelona - Eixample'
        station(2).qualitat_aire(end+1)=qualitat_aire(ii);
        station(2).codi_dtes(end+1)=codi_dtes(ii);
        station(2).zqa(end+1)=zqa(ii);
        station(2).codi_eoi(end+1)=codi_eoi(ii);
        station(2).qualitat_o3(end+1)=qualitat_o3(ii);
        station(2).hora_o3(end+1)=hora_o3(ii);
        station(2).valor_o3(end+1)=valor_o3(ii);
        station(2).qualitat_no2(end+1)=qualitat_no2(ii);
        station(2).hora_no2(end+1)=hora_no2(ii);
        station(2).valor_no2(end+1)=valor_no2(ii);
        station(2).qualitat_pm10(end+1)=qualitat_pm10(ii);
        station(2).hora_pm10(end+1)=hora_pm10(ii);
        station(2).valor_pm10(end+1)=valor_pm10(ii);
        %        station(2).generat(end+1)=generat(ii);
        station(2).limit_o3(end+1)=o3_l;
        station(2).limit_no2(end+1)=no2_l;
        station(2).limit_pm10(end+1)=pm10_l;
        station(2).generat(end+1)=datetime(generat(ii),'Format','dd/MM/yyyy H:mm');
    case 'Barcelona - Gràcia'
        station(3).qualitat_aire(end+1)=qualitat_aire(ii);
        station(3).codi_dtes(end+1)=codi_dtes(ii);
        station(3).zqa(end+1)=zqa(ii);
        station(3).codi_eoi(end+1)=codi_eoi(ii);
        station(3).qualitat_o3(end+1)=qualitat_o3(ii);
        station(3).hora_o3(end+1)=hora_o3(ii);
        station(3).valor_o3(end+1)=valor_o3(ii);
        station(3).qualitat_no2(end+1)=qualitat_no2(ii);
        station(3).hora_no2(end+1)=hora_no2(ii);
        station(3).valor_no2(end+1)=valor_no2(ii);
        station(3).qualitat_pm10(end+1)=qualitat_pm10(ii);
        station(3).hora_pm10(end+1)=hora_pm10(ii);
        station(3).valor_pm10(end+1)=valor_pm10(ii);
        %        station(3).generat(end+1)=generat(ii);
```

Davide Carlucci

```matlab
        station(3).limit_o3(end+1)=o3_l;
        station(3).limit_no2(end+1)=no2_l;
        station(3).limit_pm10(end+1)=pm10_l;
        station(3).generat(end+1)=datetime(generat(ii),'Format','dd/MM/yyyy H:mm');
    case 'Barcelona - Ciutadella'
        station(4).qualitat_aire(end+1)=qualitat_aire(ii);
        station(4).codi_dtes(end+1)=codi_dtes(ii);
        station(4).zqa(end+1)=zqa(ii);
        station(4).codi_eoi(end+1)=codi_eoi(ii);
        station(4).qualitat_o3(end+1)=qualitat_o3(ii);
        station(4).hora_o3(end+1)=hora_o3(ii);
        station(4).valor_o3(end+1)=valor_o3(ii);
        station(4).qualitat_no2(end+1)=qualitat_no2(ii);
        station(4).hora_no2(end+1)=hora_no2(ii);
        station(4).valor_no2(end+1)=valor_no2(ii);
        station(4).qualitat_pm10(end+1)=qualitat_pm10(ii);
        station(4).hora_pm10(end+1)=hora_pm10(ii);
        station(4).valor_pm10(end+1)=valor_pm10(ii);
%          station(4).generat(end+1)=generat(ii);
        station(4).limit_o3(end+1)=o3_l;
        station(4).limit_no2(end+1)=no2_l;
        station(4).limit_pm10(end+1)=pm10_l;
        station(4).generat(end+1)=datetime(generat(ii),'Format','dd/MM/yyyy H:mm');
    case 'Barcelona - Vall Hebron'
        station(5).qualitat_aire(end+1)=qualitat_aire(ii);
        station(5).codi_dtes(end+1)=codi_dtes(ii);
        station(5).zqa(end+1)=zqa(ii);
        station(5).codi_eoi(end+1)=codi_eoi(ii);
        station(5).qualitat_o3(end+1)=qualitat_o3(ii);
        station(5).hora_o3(end+1)=hora_o3(ii);
        station(5).valor_o3(end+1)=valor_o3(ii);
        station(5).qualitat_no2(end+1)=qualitat_no2(ii);
        station(5).hora_no2(end+1)=hora_no2(ii);
        station(5).valor_no2(end+1)=valor_no2(ii);
        station(5).qualitat_pm10(end+1)=qualitat_pm10(ii);
        station(5).hora_pm10(end+1)=hora_pm10(ii);
        station(5).valor_pm10(end+1)=valor_pm10(ii);
%          station(5).generat(end+1)=generat(ii);
        station(5).limit_o3(end+1)=o3_l;
        station(5).limit_no2(end+1)=no2_l;
        station(5).limit_pm10(end+1)=pm10_l;
        station(5).generat(end+1)=datetime(generat(ii),'Format','dd/MM/yyyy H:mm');
    case 'Barcelona - Palau Reial'
        station(6).qualitat_aire(end+1)=qualitat_aire(ii);
        station(6).codi_dtes(end+1)=codi_dtes(ii);
        station(6).zqa(end+1)=zqa(ii);
        station(6).codi_eoi(end+1)=codi_eoi(ii);
        station(6).qualitat_o3(end+1)=qualitat_o3(ii);
        station(6).hora_o3(end+1)=hora_o3(ii);
        station(6).valor_o3(end+1)=valor_o3(ii);
        station(6).qualitat_no2(end+1)=qualitat_no2(ii);
        station(6).hora_no2(end+1)=hora_no2(ii);
        station(6).valor_no2(end+1)=valor_no2(ii);
        station(6).qualitat_pm10(end+1)=qualitat_pm10(ii);
        station(6).hora_pm10(end+1)=hora_pm10(ii);
        station(6).valor_pm10(end+1)=valor_pm10(ii);
%          station(6).generat(end+1)=generat(ii);
        station(6).limit_o3(end+1)=o3_l;
        station(6).limit_no2(end+1)=no2_l;
        station(6).limit_pm10(end+1)=pm10_l;
        station(6).generat(end+1)=datetime(generat(ii),'Format','dd/MM/yyyy H:mm');
```

```matlab
        case 'Barcelona - Poblenou'
            station(7).qualitat_aire(end+1)=qualitat_aire(ii);
            station(7).codi_dtes(end+1)=codi_dtes(ii);
            station(7).zqa(end+1)=zqa(ii);
            station(7).codi_eoi(end+1)=codi_eoi(ii);
            station(7).qualitat_o3(end+1)=qualitat_o3(ii);
            station(7).hora_o3(end+1)=hora_o3(ii);
            station(7).valor_o3(end+1)=valor_o3(ii);
            station(7).qualitat_no2(end+1)=qualitat_no2(ii);
            station(7).hora_no2(end+1)=hora_no2(ii);
            station(7).valor_no2(end+1)=valor_no2(ii);
            station(7).qualitat_pm10(end+1)=qualitat_pm10(ii);
            station(7).hora_pm10(end+1)=hora_pm10(ii);
            station(7).valor_pm10(end+1)=valor_pm10(ii);
            %        station(7).generat(end+1)=generat(ii);
            station(7).limit_o3(end+1)=o3_l;
            station(7).limit_no2(end+1)=no2_l;
            station(7).limit_pm10(end+1)=pm10_l;
            station(7).generat(end+1)=datetime(generat(ii),'Format','dd/MM/yyyy H:mm');
        case 'Barcelona - Observ Fabra'
            station(8).qualitat_aire(end+1)=qualitat_aire(ii);
            station(8).codi_dtes(end+1)=codi_dtes(ii);
            station(8).zqa(end+1)=zqa(ii);
            station(8).codi_eoi(end+1)=codi_eoi(ii);
            station(8).qualitat_o3(end+1)=qualitat_o3(ii);
            station(8).hora_o3(end+1)=hora_o3(ii);
            station(8).valor_o3(end+1)=valor_o3(ii);
            station(8).qualitat_no2(end+1)=qualitat_no2(ii);
            station(8).hora_no2(end+1)=hora_no2(ii);
            station(8).valor_no2(end+1)=valor_no2(ii);
            station(8).qualitat_pm10(end+1)=qualitat_pm10(ii);
            station(8).hora_pm10(end+1)=hora_pm10(ii);
            station(8).valor_pm10(end+1)=valor_pm10(ii);
            %        station(8).generat(end+1)=generat(ii);
            station(8).limit_o3(end+1)=o3_l;
            station(8).limit_no2(end+1)=no2_l;
            station(8).limit_pm10(end+1)=pm10_l;
            station(8).generat(end+1)=datetime(generat(ii),'Format','dd/MM/yyyy H:mm');
        otherwise
            disp(['Error @', num2str(ii),' iteration, because of',cabin(ii)])   % Displaying on screen if a different cabin, from
the ones tabulated, is detected
    end

end

station=station(1:8);   % Deleting the last row of the station struct

validity=zeros(length(station),3); % Checking if each station can detect all the pollutants
for kk=1:length(station)
    if(sum(isnan(station(kk).valor_o3(1,:)))==length(station(kk).valor_o3(1,:)))    % Checking if each station can detect
the O3
        validity(kk,1)=0;
    else
        validity(kk,1)=1;
    end

    if(sum(isnan(station(kk).valor_no2(1,:)))==length(station(kk).valor_no2(1,:)))  % Checking if each station can
detect the NO2
        validity(kk,2)=0;
    else
        validity(kk,2)=1;
```

Davide Carlucci

```matlab
    end

    if(sum(isnan(station(kk).valor_pm10(1,:)))==length(station(kk).valor_pm10(1,:)))% Checking if each station can
detect the PM10
        validity(kk,3)=0;
    else
        validity(kk,3)=1;
    end
end

o3_validity=sum(validity(:,1));
no2_validity=sum(validity(:,2));
pm10_validity=sum(validity(:,3));
```

Align the weather data

```matlab
dd=1;

while (day1(dd)<=station(1).generat(1))

    dd=dd+1;
end
dd=dd-1;
ll=ceil((length(station(1).generat())+1)/24);

bb=1;
while (day2(bb)<=station(1).generat(1))

    bb=bb+1;
end
bb=bb-1;
mm=ceil((length(station(1).generat())+1)*2);
```

Plot of the results

```matlab
% Enable the following part to plot the weather data

% figure(1) yyaxis right bar(day1(dd:dd+ll),prec1(dd:dd+ll),'DisplayName','precipitation','LineWidth',1)
ylabel('Precipitations [mm/day]') ylim([0 max(prec1(dd:dd+ll+10))]) hold on

%figure(2) yyaxis right bar(day1(dd:dd+ll),prec1(dd:dd+ll),'DisplayName','precipitation','LineWidth',1)
ylabel('Precipitations [mm/day]') ylim([0 max(prec1(dd:dd+ll+10))]) hold on

%figure(3) yyaxis right bar(day1(dd:dd+ll),prec1(dd:dd+ll),'DisplayName','precipitation','LineWidth',1)
ylabel('Precipitations [mm/day]') ylim([0 max(prec1(dd:dd+ll+10))]) hold on
```

```matlab
for jj=1:length(station)

    if(validity(jj,1)==1)
        figure(1)
%        yyaxis left
        plot(station(jj).generat(1,:),station(jj).valor_o3(1,:),'DisplayName',cabin(jj))
        hold on
    end
```

```matlab
    if(validity(jj,2)==1)
        figure(2)
%         yyaxis left
        plot(station(jj).generat(1,:),station(jj).valor_no2(1,:),'DisplayName',cabin(jj))
        hold on
    end

    if(validity(jj,3)==1)
        figure(3)
%         yyaxis left
        plot(station(jj).generat(1,:),station(jj).valor_pm10(1,:),'DisplayName',cabin(jj))
        hold on
    end

    if (jj==length(station))    % Adding title, labels, grid, and limit at the last iteration
        figure(1)
        plot(station(jj).generat(1,:),station(jj).limit_o3(1,:),'DisplayName','O_3 limit','LineWidth',1.5)
        title(['O_3 concentration ',datestr(station(jj).generat(1),'mmmm yyyy')])
        xlabel('Day')
%         yyaxis left
        ylabel('Concentration [µg/m³]')
        %ylim([0 (max(max(station(1,:).valor_o3(1,:)),o3_l)+10)])
        grid minor
        legend('show','Location','southoutside','NumColumns',2)

        figure(2)
        plot(station(jj).generat(1,:),station(jj).limit_no2(1,:),'DisplayName','NO_2 limit','LineWidth',1.5)
        title(['NO_2 concentration ',datestr(station(jj).generat(1),'mmmm yyyy')])
        xlabel('Day')
%         yyaxis left
        ylabel('Concentration [µg/m³]')
        %ylim([0 (max(max(station(1,:).valor_no2(1,:)),no2_l)+10)])
        grid minor
        legend('show','Location','southoutside','NumColumns',2)

        figure(3)
        plot(station(jj).generat(1,:),station(jj).limit_pm10(1,:),'DisplayName','PM10 limit','LineWidth',1.5)
        title(['PM10 concentration ',datestr(station(jj).generat(1),'mmmm yyyy')])
        xlabel('Day')
%         yyaxis left
        ylabel('Concentration [µg/m³]')
        %ylim([0 (max(max(station(1,:).valor_pm10(1,:)),pm10_l)+10)])
        grid minor
        legend('show','Location','southoutside','NumColumns',2)
    end
end

% Enable the following part to plot the weather data

% figure(1)
% yyaxis right
% bar(day1(dd:dd+ll),prec1(dd:dd+ll),'DisplayName','precipitation1','LineWidth',1)
% ylabel('Precipitations [mm/day]')
% ylim([0 max(prec1(dd:dd+ll)+5)])
% ax=gca;
% ax.YColor='k';
% hold on
%
% figure(2)
% yyaxis right
```

```
% bar(day1(dd:dd+ll),prec1(dd:dd+ll),'DisplayName','precipitation','LineWidth',1)
% ylabel('Precipitations [mm/day]')
% ylim([0 max(prec1(dd:dd+ll)+5)])
% ax=gca;
% ax.YColor='k';
% hold on
%
% figure(3)
% yyaxis right
% plot(day2(bb:bb+mm),prec2(bb:bb+mm),'DisplayName','precipitation2','LineWidth',3)
% hold on
% bar(day1(dd:dd+ll),prec1(dd:dd+ll),'DisplayName','precipitation','LineWidth',1)
% ylabel('Precipitations [mm/day]')
% ylim([0 max(prec1(dd:dd+ll)+5)])
% ax=gca;
% ax.YColor='k';
% hold on
```


Figure — O$_3$ concentration November 2018

Davide Carlucci

NO$_2$ concentration November 2018

PM10 concentration November 2018

Davide Carlucci
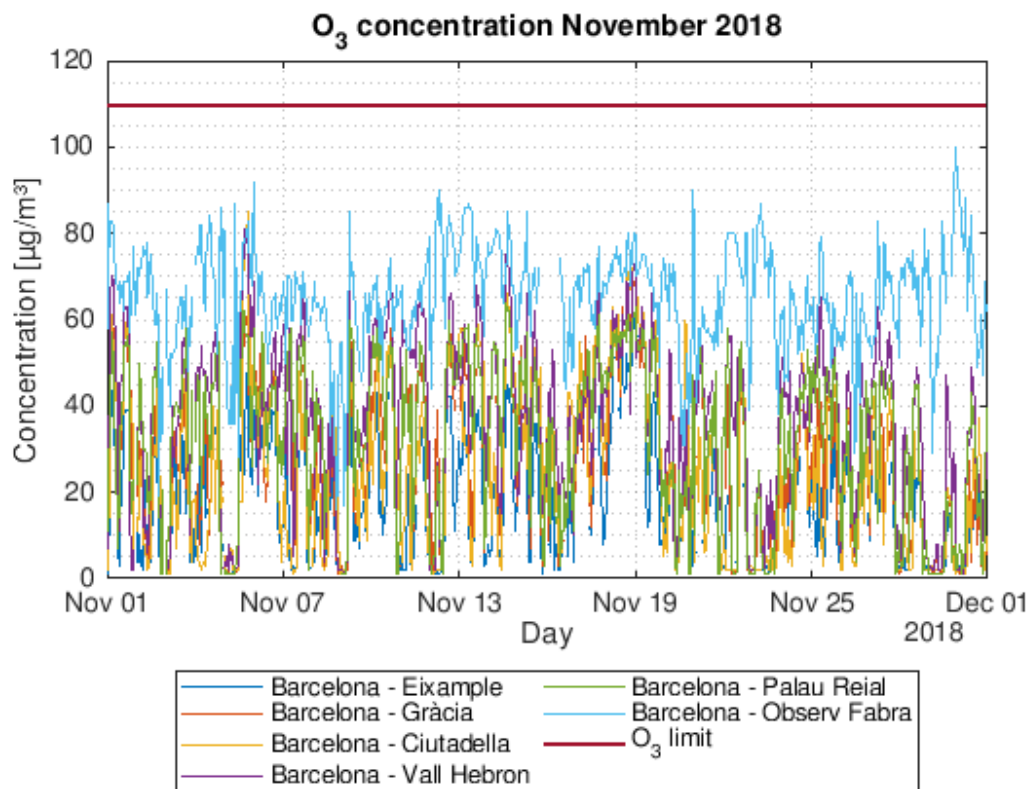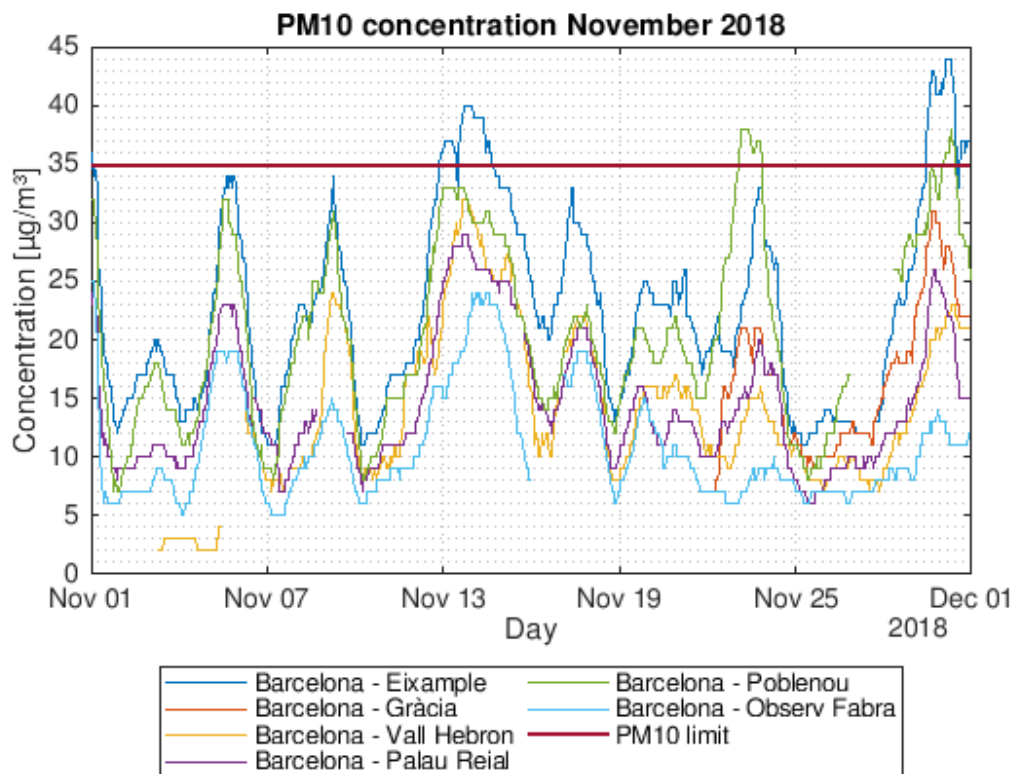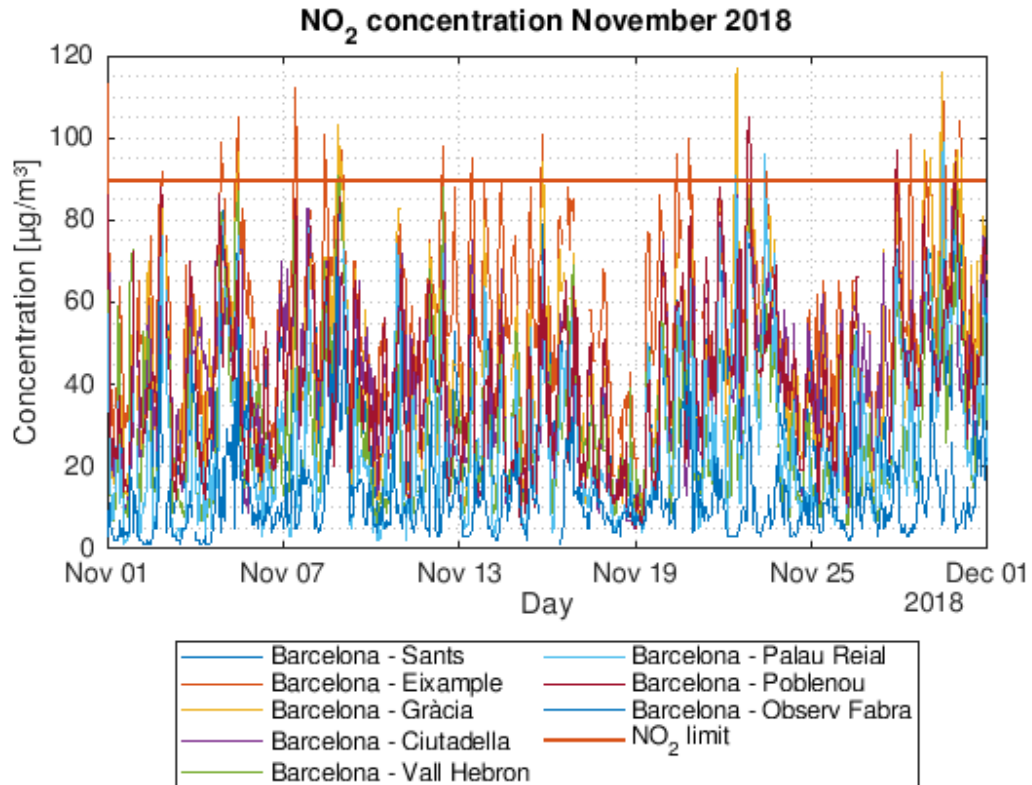
Execution time calculation & Screen message

```
disp(['Data analysed for ',datestr(station(jj).generat(1),'mmmm yyyy')])  % Displaying on screen the month analysed
time_script_execution=toc;
disp(['Script execution time: ', num2str(time_script_execution),' s'])  % Displaying on screen the execution time
disp(['O3 limit exceeded ',num2str(o3_index),' times out of ',num2str(ceil(length(generat)*o3_validity/8)),'
measurements from ',num2str(o3_validity),' stations'])
disp(['NO2 limit exceeded ',num2str(no2_index),' times out of ',num2str(ceil(length(generat)*no2_validity/8)),'
measurements from ',num2str(no2_validity),' stations'])
disp(['PM10 limit exceeded ',num2str(pm10_index),' times out of ',num2str(ceil(length(generat)*pm10_validity/8)),'
measurements from ',num2str(pm10_validity),' stations'])
%----------------------------------------------------------------%
```

Data analysed for November 2018

Script execution time: 40.3658 s

O3 limit exceeded 0 times out of 4308 measurements from 6 stations

NO2 limit exceeded 66 times out of 5744 measurements from 8 stations

PM10 limit exceeded 115 times out of 4308 measurements from 6 stations

Notes

Air pollution data obtained from: https://opendata-ajuntament.barcelona.cat/data/en/dataset/qualitat-aire-detall-bcn

MATLAB R2019a ONLINE has been used. Check for compatibility before running the script

Script created by Davide Carlucci davidecarlucci95@gmail.com

Published with MATLAB® R2019a (ONLINE version)

APPENDIX B – Simulations tables

Table 1 (Reference case)

Speed [km/h]	C_d [-]	Area [m]	C_d A [m]
10	0.323	1.344	0.434
20	0.319	1.344	0.429
30	0.317	1.344	0.427
40	0.317	1.344	0.426
50	0.316	1.344	0.425
60	0.316	1.344	0.424
70	0.315	1.344	0.424
80	**0.315**	**1.344**	**0.424**
90	0.315	1.344	0.423

Table 2.a (Case A)

C_d [%]		Speed	
Distance (x_d)	30 km/h	50 km/h	80 km/h
0.0 m	108%	110%	111%
0.3 m	79%	81%	82%
0.6 m	58%	60%	61%
0.9 m	51%	52%	53%

Table 2.b (Case A)

C_d [-]		Speed	
Distance (x_d)	30 km/h	50 km/h	80 km/h
0.0 m	0.660	0.662	0.664
0.3 m	0.567	0.571	0.574
0.6 m	0.502	0.505	0.508
0.9 m	0.478	0.480	0.482

Table 2.c (Case A)

C_d A [m]		Speed	
Distance (x_d)	30 km/h	50 km/h	80 km/h
0.0 m	0.985	0.989	0.993
0.3 m	0.839	0.844	0.849
0.6 m	0.743	0.748	0.752
0.9 m	0.712	0.716	0.719

Table 2.d (Case A)

Δp [Pa]		Speed	
Distance (x_d)	30 km/h	50 km/h	80 km/h
0.0 m	11.5	31.5	79.3
0.3 m	11.0	29.5	73.0
0.6 m	9.7	26.2	65.5
0.9 m	8.2	22.7	57.5

Davide Carlucci

Table 2.e (Case A)

$\dot{V}$ [m²/h]	Speed		
Distance (x_d)	30 km/h	50 km/h	80 km/h
0.0 m	58.9	134.0	282.3
0.3 m	79.6	177.1	356.8
0.6 m	68.1	152.4	309.8
0.9 m	55.5	123.9	253.4

Table 3.a (Case B)

C_d [-]	Distance (y_d)		
Distance (x_d)	0.00 m	0.05 m	0.10 m
0.0 m	0.664	0.628	0.551
0.3 m	0.574	0.587	0.518
0.6 m	0.508	0.545	0.487
0.9 m	0.482	0.521	0.476

Table 3.b (Case B)

C_d [%]	Distance (y_d)		
Distance (x_d)	0.00 m	0.05 m	0.10 m
0.0 m	111%	99%	75%
0.3 m	82%	86%	64%
0.6 m	61%	73%	55%
0.9 m	53%	65%	51%

Table 3.c (Case B)

$C_d A$ [m]	Speed		
Distance (x_d)	30 km/h	50 km/h	80 km/h
0.0 m	0.993	0.947	0.831
0.3 m	0.849	0.885	0.782
0.6 m	0.752	0.822	0.735
0.9 m	0.719	0.785	0.717

Table 3.d (Case B)

Δp [Pa]	Distance (y_d)		
Distance (x_d)	0.00 m	0.05 m	0.10 m
0.0 m	79.3	114.2	124.2
0.3 m	73.0	99.0	117.5
0.6 m	65.5	86.3	112.2
0.9 m	57.5	84.0	111.7

Table 3.e (Case B)

$\dot{V}$ [m²/h]	Distance (y_d)		
Distance (x_d)	0.00 m	0.05 m	0.10 m
0.0 m	282.3	190.4	233.3
0.3 m	356.8	175.7	219.1
0.6 m	309.8	169.5	213.1
0.9 m	253.4	197.4	221.1

Table 4.a (case C)

Case C	
C_d	0.369
A	1.344 m
$C_d A$	0.496 m
Δp	77.3 Pa
$\dot{V}$	1708.8 m²/h

Davide Carlucci

Table 5.a (Case D)   Table 6.a (Case E)

Case D	
C_d	0.404
A	2.144 m^2
C_dA	0. 866 m^2
Δp	40.8 Pa
$\dot{V}$	83.1 m^3/h

Case E	
C_d	0.366
A	2.144 m^2
C_dA	0. 784 m^2
Δp	40.0 Pa
$\dot{V}$	112.3 m^3/h

Davide Carlucci